Proglacial lake evolution and outburst flood hazard at Fjallsjökull glacier, southeast Iceland

Wells, Greta Hoe[1,2], Sæmundsson, Þorsteinn[1,3], Pálsson, Finnur[1], Aðalgeirsdóttir, Guðfinna[1], Magnússon, Eyjólfur[1], Hermanns, Reginald L.[4,5], Guðmundsson, Snævarr[6]

[1] Institute of Earth Sciences, University of Iceland, Reykjavík, 101, Iceland
[2] School of Geosciences, University of Edinburgh, Edinburgh, EH8 9XP, UK
[3] Faculty of Life and Environmental Sciences, University of Iceland, Reykjavík, 101, Iceland
[4] Geological Survey of Norway, Trondheim, 7040, Norway
[5] Norwegian University of Science and Technology, Trondheim, 7491, Norway
[6] South East Iceland Nature Research Center, Höfn, 780, Iceland

Correspondence to: Greta H. Wells (ghwells@hi.is)

Abstract. Glacier retreat is projected to increase with future climate warming, elevating the risk of mass movement-triggered glacial lake outburst floods (GLOFs). These events are an emerging yet understudied hazard in Iceland, including at Fjallsjökull, an outlet glacier of the Vatnajökull ice cap in southeast Iceland. A multibeam sonar scanner survey revealed that the proglacial Fjallsárlón lake significantly expanded from 1945 to 2021. If recent glacier terminus retreat rates continue, Fjallsárlón will reach its maximum extent around 2110, more than doubling in surface area and tripling in volume. The lake will occupy two overdeepened basins with a maximum depth of ~210 m, which will likely increase terminus melting and calving rates—and thus glacier retreat—as well as potentially float the glacier tongue. Three zones on the valley walls above Fjallsjökull have high topographic potential of sourcing rock falls or avalanches that could enter Fjallsárlón and generate displacement waves or GLOFs, significantly impacting visitors and infrastructure at this tourism site. This study provides input data for risk assessments and mitigation strategies at Fjallsjökull; a template for investigating this hazard at other proglacial lakes in Iceland; and field data to advance understanding of overdeepenings and lake–terminus interactions in proglacial lakes worldwide.

1. Introduction and aims

Glaciers worldwide have retreated rapidly over the past century, and this rate is projected to continue with future climate warming (Hock et al., 2019; Zemp et al., 2019; Marzeion et al., 2020; Hugonnet et al., 2021; Rounce et al., 2023). Proglacial lakes often form in front of retreating glacier termini, particularly where ice has eroded overdeepened troughs into bedrock and sediment, and these lakes are growing in size and number as glaciers retreat worldwide (Cook and Swift, 2012; Carrivick and Tweed, 2013; Haeberli et al., 2016; Shugar et al., 2020; Zhang et al., 2024). Proglacial lakes can drain suddenly and catastrophically in jökulhlaups (also referred to as glacial lake outburst floods or GLOFs) if their dams are breached by displacement waves generated by a mass movement event—such as a rapid rock slope failure, ice avalanche, or landslide—

that enters the lake (Evans and Cla..., 994; Westoby et al., 2014a; Haeberli et al., 2017; ...son et al., 2018). These mass

35   movements may be triggered by paraglacial processes, such as glacier debuttressing, permafrost thaw, freeze–thaw activity, or stress adjustments from post-glacial crustal unloading and rebound, as well as seismic activity, extreme precipitation or snowmelt events, and ice crevassing and avalanching (Gruber and ...berli, 2007; McColl, 2012; Stoffel and Huggel, 2012; Korup and Dunning, 2015; Krautblatter and Leith, 2015; Deline et al., 2015, 2022; Ballantyne, 2022). Moreover, these processes can act in positive feedback loops, as glacial lake deepening increases terminus melt and calving rates (Carrivick et

40   al., 2020; Sutherland et al., 2020), and glacial lake expansion increases the lake surface area where mass movements can enter and the water volume that can be displaced (Emmer et al., 2020).

GLOFs can significantly impact landscapes and societies far downstream of the source lake, leaving a geomorphologic legacy that persists over long time scales (Carrivick and Tweed, 2016; Larsen and Lamb, 2016; Wells et al., 2022; Emmer, 2023; Lützow et al., 2023; Morey et al., 2024). GLOFs may also trigger hazard cascades by entraining material

45   to transform into debris flows, undercutting channel banks to increase likelihood of subsequent collapse, and depositing material to dam new lakes at risk of draining (Korup and Tweed, 2007; Worni et al., 2014; Allen et al., 2022; Geertsema et al., 2022). Mass movements into proglacial lakes have triggered GLOFs across the globe, including in the Himalaya–Hindu Kush (Richardson and Reynolds, 2000), Andes (Hubbard et al., 2005), Patagonia (Harrison et al., 2006), Canadian Cordillera (Clague and Evans, 2000), and Iceland (Kjartansson, 1967), as well as tsunamis in marine fjords in Greenland (Svennevig et al., 2020),

50   Norway (Hermanns et al., ...), and Alaska (Higman et al., 2018).

Projected climate warming is expected to increase glacier retreat, proglacial lake expansion, and paraglacial activity in Iceland, heightening the threat of mass movement-triggered GLOFs, though this emerging hazard remains understudied. Though jökulhlaups occur more frequently in Iceland than nearly anywhere else on Earth, most have been triggered by subglacial volcanic and geothermal activity (Björnsson, 2002; Dunning et al., 2013; Carrivick and Tweed, 2019; Magnússon

55   et al., 2021) or ice dam flotation or failure (Thorarinsson, 1939; Roberts et al., 2005). Rapid glacier retreat and thinning is occurring in Iceland, with a 16 ± 4% decrease in ice volume since 1890 (Aðalgeirsdóttir et al., 2020; Belart et al., 2020; Hannesdóttir et al., 2020) and a projected additional loss of at least 20% by 2100 for its largest ice caps (Flowers et al., 2005; Aðalgeirsdóttir et al., 2011; Schmidt et al., 2020; Compagno et al., 2021; Rounce et al., 2023). Proglacial lakes have expanded since they began to form in the early twentieth century and now occur in front of most southern outlet glaciers at Vatnajökull,

60   Iceland's largest ice cap (Guðmundsson et al., 2019). Mass movements partly attributed to paraglacial processes have fallen onto several outlet glaciers in Iceland in the past century, including Steinsholtsjökull (1967), an outlet glacier of the Eyjafjallajökull ice cap (Kjartansson, 1967), Jökulsárgilsjökull (1972) (Sigurðsson and Williams, 1991) and Tungnakvíslarjökull (2003), outlet glaciers of the Mýrdalsjökull ice cap, and Morsárjökull (2007) (Sæmundsson et al., 2011) and Svínafellsjökull (2013) (Ben-Yehoshua et al., 2022), outlet glaciers of the Vatnajökull ice cap (Fig. 1A and 1B); and

65   ongoing surface deformation is observed above Tungnakvíslarjökull (Lacroix et al., 2022) and Svínafellsjökull (Ben-Yehoshua et al., 2023). Despite many locations of activity, only one known mass movement has triggered a GLOF in Iceland—the

rockslide onto the Steinsholtsjökull outlet glacier in 1967, which fractured glacial ice and slid into the proglacial lake, where it generated a displacement wave that continued downstream as a flood and debris flow (Kjartansson, 1967).

70   One site with favorable conditions for mass-movement triggered GLOFs is Fjallsjökull, an outlet glacier of the Vatnajökull ice cap in southeast Iceland that is located in Vatnajökull National Park (Fig. 1C). Fjallsjökull is rapidly retreating in a steep-walled valley with an overdeepened trough and is in contact with the proglacial Fjallsárlón lake. A mass movement-triggered GLOF from Fjallsárlón could have a significant societal impact since the lake is one of Iceland's most visited glacier tourism sites—attracting more than 260,000 visitors in 2022 (Þórhallsdóttir, 2023)—and is situated ~1 km west of Route 1, which is the only land route connecting eastern and western Iceland on the south coast. This study addresses the questions:

75   how will Fjallsárlón evolve under ongoing climate warming, and how will this evolution influence GLOF risk from mass movement events into the lake? This paper: 1) presents results of a 2020 lake bathymetric survey with a multibeam sonar scanner; 2) reconstructs lake volume changes from 1945 to 2021; 3) estimates future lake and glacier evolution; and 4) identifies potential sources of mass movements and discusses resulting GLOF scenarios from Fjallsárlón.

2. Study area and background

80   Fjallsjökull is an outlet glacier of the southern part of Öræfajökull, a central volcano that lies beneath the Vatnajökull ice cap in southeast Iceland (Fig. 1B). Fjallsjökull reached its maximum historical extent in the 18th and 19th centuries (Thorarinsson, 1943; Bradwell, 2004). The glacier was connected with the Hrútárjökull outlet glacier to the south, but the ice had retreated enough to separate into two termini by 2010 (Hannesdóttir et al., 2015; Guðmundsson et al., 2019). Between ~1890 and 2010, the glacier lost ~23% of its surface area and ~35% of its volume (Hannesdóttir et al., 2015). Bedrock maps

85   from radio-echo sounding surveys show that Fjallsjökull occupies two overdeepened troughs carved into bedrock and sediment reaching up to ~205 m and ~120 m below sea level (Magnússon et al., 2012). The glacier is bounded by the Breiðamerkurfjall mountain to the north and the Ærfjall mountain to the south (Fig. 1C). Approximately 5 km from the present-day terminus, the glacier flows over a series of bedrock steps that create ice falls (Magnússon et al., 2012). Small proglacial lakes began to form in front of Fjallsjökull in 1936, one of which eventually became Fjallsárlón (Howarth and Price, 1969; Guðmundsson et al.,

90   2019). Since its first appearance in aerial photographs and maps in 1945, the lake surface area expanded from ~0.5 km² to ~3.7 km² in 2018 (Guðmundsson et al., 2019). Point surveys conducted with a weighted rope (and echo-sounder in 1966) revealed a maximum lake depth of 45 m in 1951, 58 m in 1966, 66 m in 2006, and 119 m in 2016 (Howarth and Price, 1969; Magnússon et al., 2007; Guðmundsson et al., 2019). A neighboring glacial lake, Breiðárlón, drains into Fjallsárlón via the Breiðá river. Fjallsárlón's outlet is the Fjallsá river, which flows for ~8 km southeast across a sandur to the Atlantic Ocean (Fig. 1C).
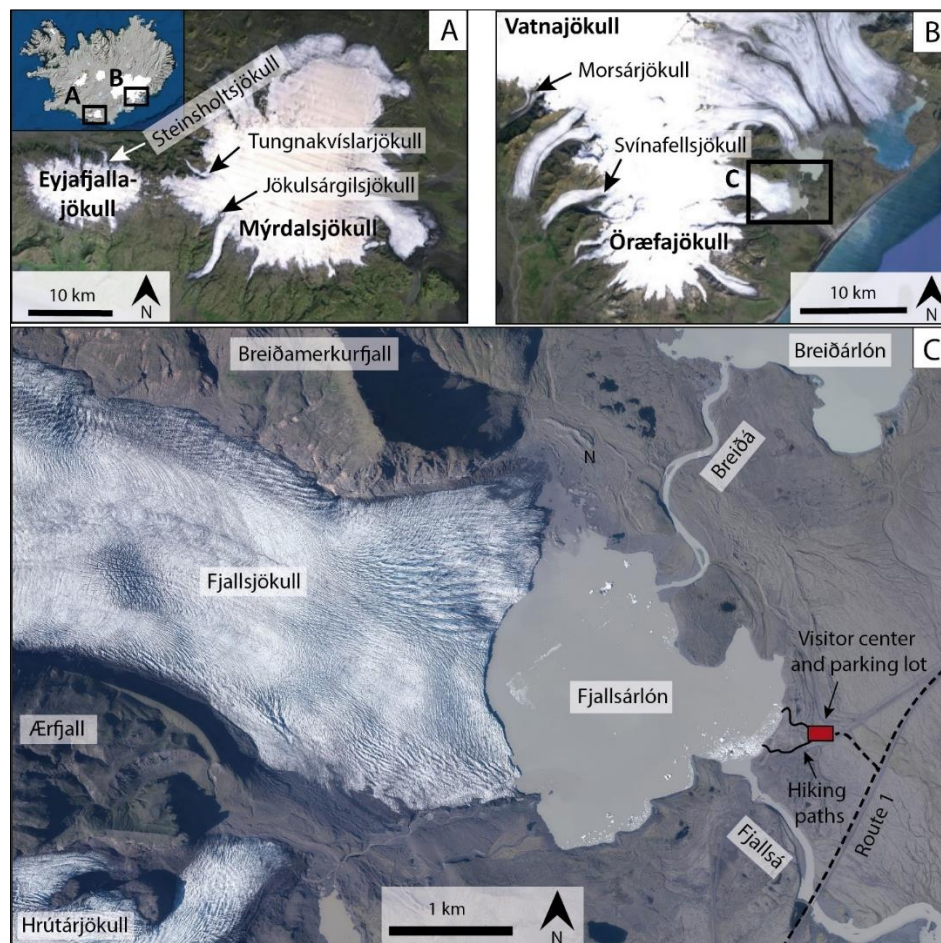
Figure 1. Map of study area and selected locations of historic mass movements onto glaciers in Iceland that are mentioned in the main text. (A) Mýrdalsjökull and Eyjafjallajökull ice caps (Google Earth basemap); (B) Öræfajökull volcano beneath Vatnajökull ice cap (Google Earth basemap); (C) Fjallsjökull glacier and Fjallsárlón lake (basemap photo from 2021 (Loftmyndir ehf., 2022)).

The glacier foreland contains landform assemblages characteristic of active temperate glacial landsystems, including moraines, till, hummocky terrain, and glacial and glaciofluvial sediments and deposits (Evans and Twigg, 2002; Chandler et al., 2020). Bedrock in the area is predominantly subaerially erupted basalt (formed during interglacial periods) and subglacially erupted basalt including hyaloclastite, breccia, and pillow lava (formed during glacial periods) that date to ~0.7 to 2.7 million years and older (Stevenson et al., 2006; Roberts and Gudmundsson, 2015). Some plutonic rocks also occur in Breiðamerkurfjall at the northern margin of Fjallsjökull (Hauksdóttir et al., 2021). Despite Iceland's subarctic location, regional climate is mild and maritime due to influence from the warm Irminger Current. Mean annual temperature near the glacier terminus is ~5° C (measured at the Fagurhólsmýri weather station ~20 km southwest of Fjallsárlón from 1949 to 2023), and mean annual precipitation is ~3500 mm (measured at the Kvísker station approximately 6 km southwest of Fjallsárlón from 1962 to 2011) (Icelandic Meteorological Office, 2024).

3. Methods

3.1. Bathymetric survey and bed DEM

A bathymetric survey was conducted in August 2020 using a Teledyne RESON SeaBat T20-P multibeam sonar scanner (420 kHz) attached to a small, motorized boat. GNSS data was collected with a Trimble SPS-852 land survey rover on-board and RTK base station close to the lakeshore, yielding a relative accuracy of ± 3 cm in vertical and horizontal. Multibeam sonar scanner results were corrected for sound wave velocity changes based on temperature and depth. Lake surface elevation was measured at a point along the shoreline at the time of the bathymetric survey with a Trimble TCS-3 (Trimble 852 reference station) and a survey stick and reported as 5 m above sea level (m a.s.l.) following correction for above-geoid height (ISN93 coordinate system).

To create a continuous topographic digital elevation model (DEM) of the Fjallsjökull area (hereafter referred to as the bed DEM), three datasets were combined: 1) bathymetric data from the multibeam sonar survey; 2) subglacial topography measured with radio-echo sounding surveys by the Institute of Earth Sciences, University of Iceland in 2005–2006, interpolated from point measurements (vertical uncertainty of point measurements ± 20 m) (Magnússon et al., 2012); and 3) ÍslandsDEM, a DEM of subaerial topography created from an airborne lidar survey in 2010–2011 (vertical uncertainty <0.5 m) (Jóhannesson et al., 2013; Landmælingar Íslands, 2021). These datasets were mosaicked together using Surfer®, version 13 (Golden Software, LLC, 2015), with which all subsequent data processing and calculations were carried out. Since the bathymetric survey could not cover the entire lake extent due to shallow water, floating icebergs, and proximity to the calving terminus, data gaps between the surveyed area and 2021 lakeshore outline were interpolated via kriging.

3.2. Glacier terminus evolution

Fjallsjökull terminus positions for eight time steps between 1890 and 2019 were retrieved from the Icelandic Glacier Web Portal (Hannesdóttir and Guðmundsson, 2024) and originally derived from remote sensing imagery, lidar DEMs, maps, and field measurements (Hannesdóttir et al., 2015, 2020; Guðmundsson et al., 2019). The 2021 terminus was manually digitized from an aerial photograph from Loftmyndir ehf. (Loftmyndir ehf., 2022) (Fig. 2). Glacier terminus retreat rates were calculated using the rectilinear box method, which captures Fjallsjökull's asymmetric terminus shape (Lea et al., 2014; Dell et al., 2019). Following the methodology presented in Moon and Joughin (2008) and Howat and Eddy (2011), we drew a rectangular box that included maximum terminus locations between 1890 and 2021 and had an arbitrary boundary roughly 500 m up-glacier from the minimum (2021) terminus position. For each year, we calculated glacier-covered area within the box; measured the areal differences between successive time steps; and divided area change by box width (approximately perpendicular to glacier flow line) to estimate average horizontal terminus retreat distance during the time interval. Finally, we divided retreat distances by the number of years in the time interval to estimate the average annual horizontal retreat rate across the terminus. Future glacier terminus retreat rate was estimated using the annual average retreat rate from 2000–2021, which captures glacier response to an atmospheric temperature increase in Iceland after ~1995, a trend that we expect to

continue with future climate warming (Björnsson et al., 2013; Aðalgeirsdóttir et al., 2020). This rate was used to estimate terminus positions at decadal intervals from 2030–2120, assuming that the 2000–2021 retreat rate continues and that all parts of the terminus retreat at the same rate.
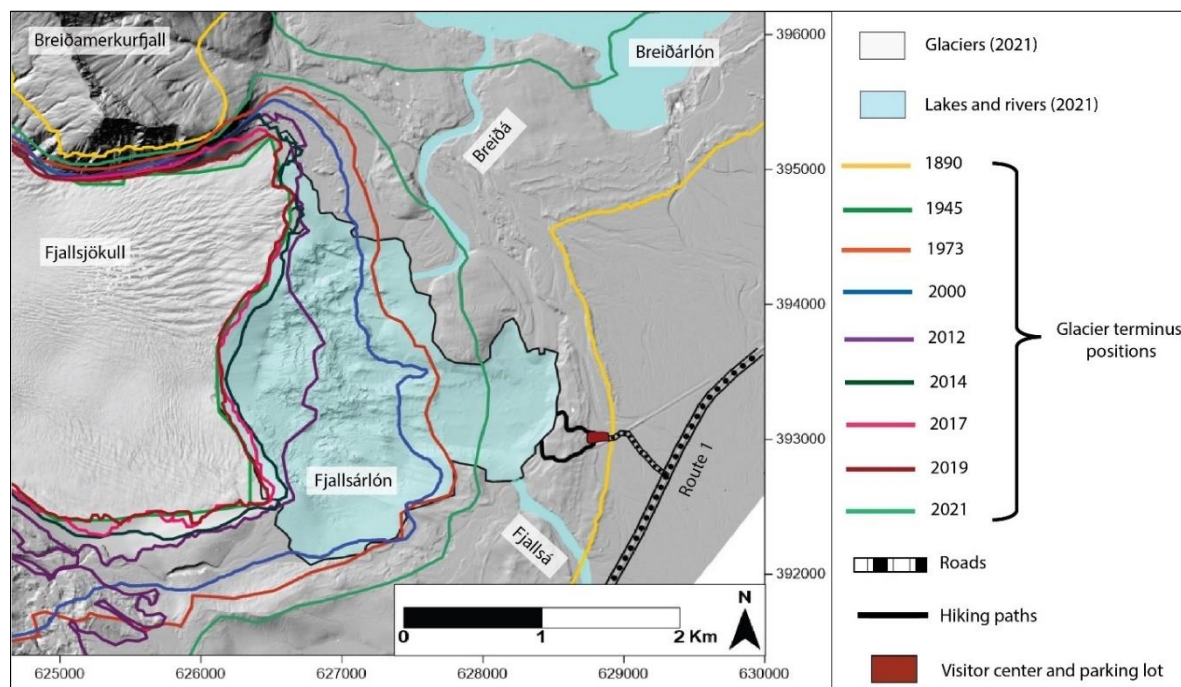
Figure 2. Fjallsjökull terminus positions at nine time steps between 1890 and 2021 (glacier outlines obtained from Hannesdóttir and Guðmundsson (2024) and a 2021 aerial photo from Loftmyndir ehf. (2022)). ÍslandsDEM basemap (Landmælingar Íslands, 2021).

3.3. Lake surface area and volume calculations

Lake surface area and volume were calculated for 20 time steps between 1945 and 2021 using the bed DEM and digitized lake outlines. Outlines for 1945–2018 were obtained from Guðmundsson et al. (2019) and were originally derived from aerial photographs, satellite images, lidar DEMs, maps, and field observations. The 2021 outline was manually digitized from an aerial photograph from Loftmyndir ehf. (Loftmyndir ehf., 2022) (Fig. 3). Though there are no reported lake surface elevation measurements prior to 2020, digitized lake outlines show that the eastern, northern, and southern shorelines have remained in similar positions since the first aerial photograph of Fjallsárlón was taken in 1945, indicating a relatively stable surface elevation; thus, we used the 2020 measured lake surface elevation to estimate future evolution. Future lake extents were estimated for ten time steps between 2030 and 2120 by digitizing the outline of the 2021 lake shoreline, then extending it up-valley along the 5 m a.s.l. contour line to each projected glacier terminus position, assuming that 2020 lake surface elevation will remain constant. Lake surface area and volume were then calculated for each estimated future lake outline using the bed DEM.
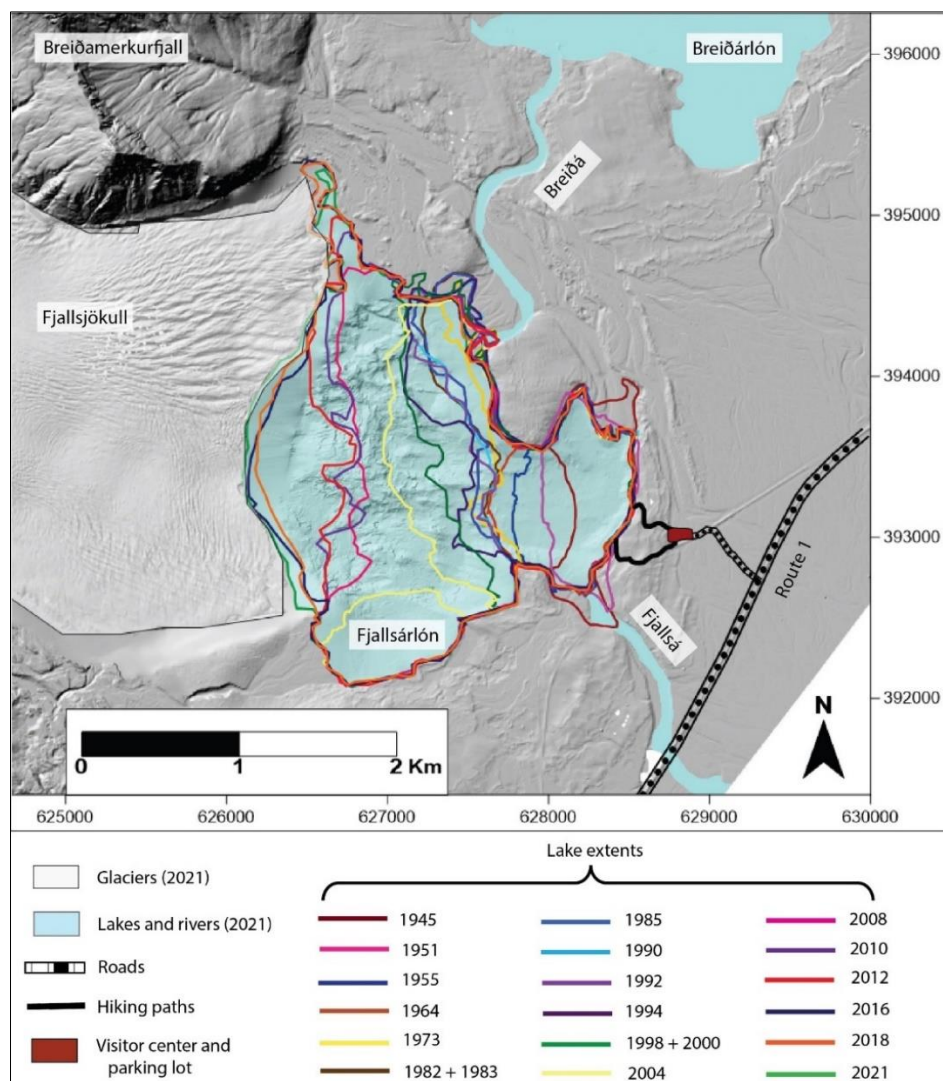
Figure 3. Fjallsárlón lake extents for 20 time steps between 1945 and 2021 (lake outlines obtained from Guðmundsson et al. (2019) and a 2021 aerial photo from Loftmyndir ehf. (2022)). ÍslandsDEM basemap (Landmælingar Íslands, 2021).

3.4. Mass movement potential and glacial lake outburst flood threat

Slope angle and vertical elevation of the valley walls above Fjallsjökull were mapped using the ÍslandsDEM basemap (Landmælingar Íslands, 2021) in ArcGIS Pro (version 3.2.0) and the bed DEM. To identify areas with a higher potential of sourcing a mass movement, we delineated zones that met two criteria: 1) slope angles >30°, which numerous studies have defined as a critical threshold for slopes more prone to failure (Romstad et al., 2009; Allen et al., 2019; Emmer et al., 2020; Penna et al., 2022); and 2) vertical relief >200 m, which are expected to yield enough material to significantly impact the glacier or lake below (Böhme et al., 2022). In each of the identified zones, we evaluated the potential of a mass movement

reaching the glacial lake—and thus potentially triggering a GLOF—by measuring four parameters based on glacier and lake

170   positions in 2021 and when the lake has reached its estimated maximum future extent: 1) maximum vertical height (vertical distances from the highest point in the zone to the 2021 glacier surface at the zone base and to the assumed future lake surface of 5 m a.s.l.); 2) horizontal travel distance (horizontal distances from the midpoint of the zone's lowest boundary to the 2021 glacier terminus and estimated future lakeshore along the shortest straight-line path); 3) H/L ratio (H = maximum height difference between the highest zone point and the lowest point of the mass movement deposit, assumed to be the lake surface

175   elevation of 5 m a.s.l.; L = horizontal length between the highest zone point and the lowest deposit point along the estimated flow path); and 4) angle of reach (fahrböschung), defined as $\tan^{-1}$ (H/L) (Hermanns et al., 2022). We also measured the horizontal distance between the highest and lowest zone boundaries (Fig. 4). Taken together, these measurements provide a first order assessment of the topographic potential for valley walls to produce mass movements that could trigger a GLOF from Fjallsárlón (Hermanns et al., 2013; Allen et al., 2019; Emmer et al., 2020; Zheng et al., 2021). We also calculated glacier

180   surface gradient along the central flow line from below the ice fall to the 2021 terminus using a 2021 glacier DEM (Belart and Magnússon, 2024). Finally, we looked for evidence of previous mass movement events in aerial photos from 2003, 2015, 2019, and 2021 (Loftmyndir ehf., 2022) and 1982 and 1998 (Landmælingar Íslands, 2022).
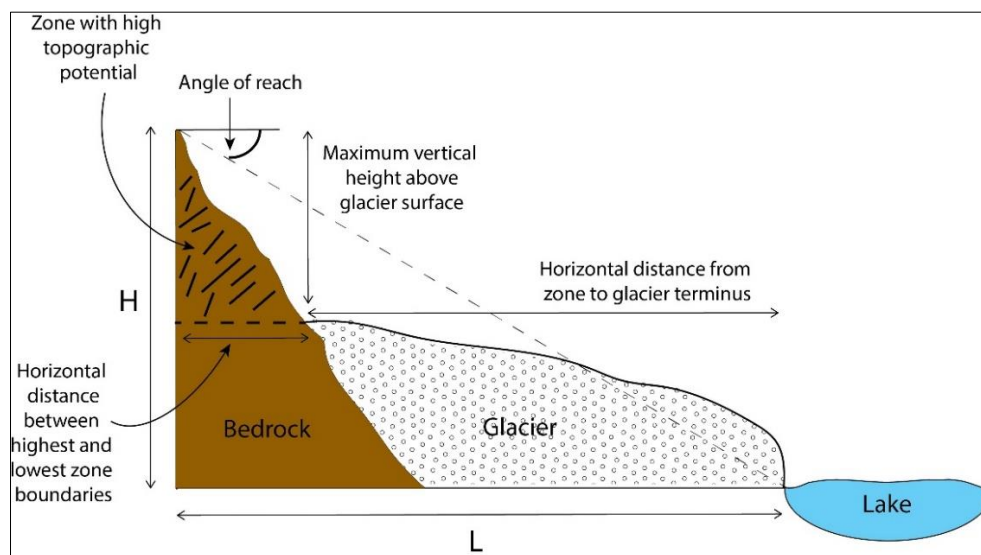
Figure. 4. Schematic diagram of topographic parameters measured to assess the potential of a mass movement event entering a
185   **glacial lake.**

4. Results

4.1. Topography of the Fjallsjökull area

The bed DEM reveals two overdeepened troughs (Fig. 5). In 2021, the southern trough was occupied partly by Fjallsárlón and partly by Fjallsjökull and reached a maximum depth of 125 m below sea level. The second trough, which is
190 located at the northern valley margin beneath Breiðamerkurfjall, reaches up to 205 m below sea level and is currently under Fjallsjökull, with the deepest point ~1.3 km from the 2021 terminus (Magnússon et al., 2012). A higher-elevation ridge reaching up to ~20 m below sea level separates the two overdeepenings. Maximum lake depth increased from 32 m in 1945 to 128 m since 2016, when Fjallsjökull retreated into the deepest section of the southern trough (Table 1). Lake depths derived from the bathymetric sonar survey generally correspond well with point depth measurements taken in 2016, as well as radio-
195 echo sounding results from 2005–2006 in the area that was covered by ice at the time of the survey but is now in the lake.

Figure 5. Bed DEM showing overdeepened basins and projected future evolution of Fjallsárlón extents and Fjallsjökull terminus positions from 2030–2120, assuming continuation of 2000–2021 terminus retreat rate (38 m yr⁻¹) and 2020 lake surface elevation (5 m a.s.l.).

4.2. Glacier terminus change, 1890–2021

Fjallsjökull retreated 2.7 km from its Little Ice Age position in ~1890 to 2021, which averages to a rate of ~20 meters per year (m a^{-1}). However, terminus retreat rates have varied significantly during different time intervals, averaging 23 m a^{-1} from 1890–1945, 42 m a^{-1} from 2000–2012, 81 m a^{-1} from 2012–2014, and 11 m a^{-1} from 2019–2021. The average annual terminus retreat rate from 2000–2021 was 38 ± 0.5 m a^{-1} (Table 1). Terminus retreat horizontal uncertainties were derived from those reported by Hannesdóttir et al. (2020) for selected terminus positions (or, where our mapped terminus year did not correspond, uncertainties for the closest year). Calculated retreat depends on methodology and measurement location; for example, Hannesdóttir et al. (2015) reported 500 m of total retreat at Fjallsjökull from 1973–2010 based on a reference point on the land-terminating glacier, while Dell et al. (2019) calculated 870 m of retreat during the same time interval for the glacier's lake-terminating portion, with the faster rate attributed to mass loss through calving (Dell et al., 2019). For comparison, our method yields an intermediate value of ~700 m of retreat during a similar time period (1973–2012), which may be because it includes the entire glacier front (both land- and lake-terminating sections).

4.3. Lake volume and surface area changes, 1945–2021

Lake volume and surface area have increased since lake extent was first mapped in 1945 (Fig. 6). The 1945 lake had a surface area of 0.33 ± 0.010 km^2 and a volume of 0.0055 ± 0.00033 km^3. By 2021, the lake covered 3.7 ± 0.050 km^2 and contained 0.19 ± 0.0036 km^3 of water. Uncertainties were estimated by calculating surface areas and volumes for lake surface elevations of 4 m and 5 m (an interval that fits within vertical uncertainties of $< \pm 0.5$ m for sonar scanner bathymetry and lidar datasets). Surface area and volume increased during each successive time interval, with the exception of very slight decreases between 1985–1990 and 2016–2018 and no change between 1982–1983 and 1998–2000 (Fig. 6; Table 1). Past lake surface areas presented here are similar to those reported by Guðmundsson et al. (2019), and volumes closely correspond to those calculated with other datasets. Differences between sonar scanner-derived volumes of the 2018 lake and volumes estimated from radio-echo sounding surveys and weighted rope point measurements are within calculated uncertainties (Guðmundsson et al., 2019).
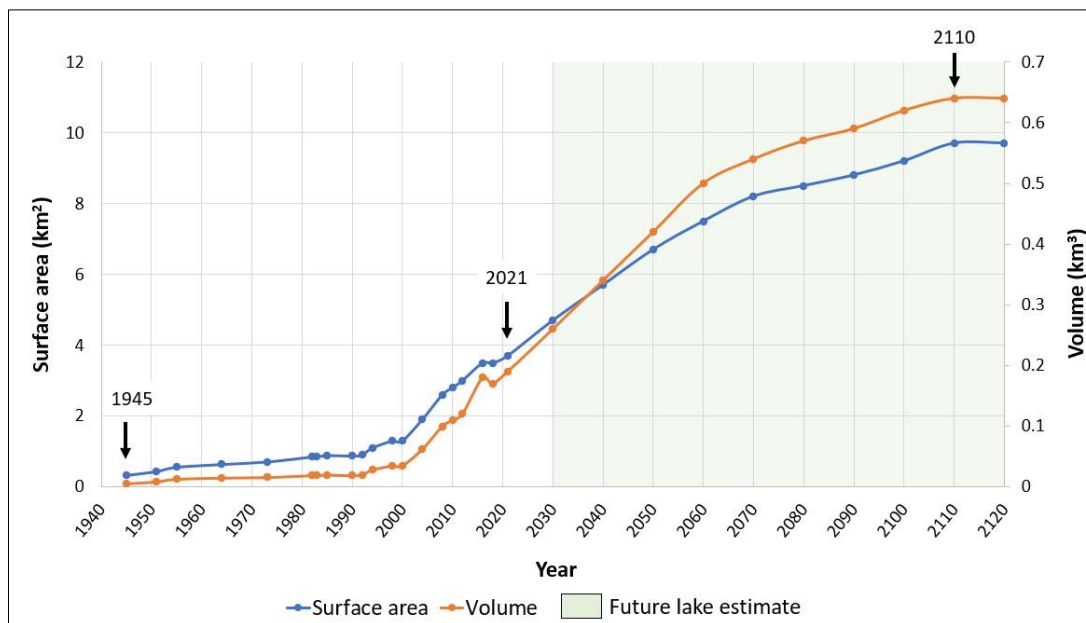
Figure 6. Fjallsárlón surface area and volume at 20 time steps from 1945–2021 and projected evolution at decadal intervals from 2030–2120. Arrows denote timing of first mapped lake extent (1945), most recent measurement (2021), and estimated future maximum lake extent (2110).

Year	Lake surface area (km²) [a]	Lake volume (km³) [a]	Maximum lake depth (m) [b]	Time interval for glacier change	Total glacier terminus retreat distance (m) within interval [c]	Average annual glacier terminus retreat rate (m a⁻¹) [d]
1890	N/A	N/A	N/A	1890-1945	1253 ± 30	23 ± 0.5
1945	0.33 ± 0.010	0.0055 ± 0.00033	32	1945-1973	410 ± 20	15 ± 0.7
1951	0.44 ± 0.0095	0.0087 ± 0.00043	37			
1955	0.56 ± 0.011	0.013 ± 0.00055	40			
1964	0.64 ± 0.011	0.015 ± 0.00063	42			
1973	0.71 ± 0.021	0.016 ± 0.00070	49	1973-2000	194 ± 15	7 ± 0.6
1982	0.85 ± 0.023	0.019 ± 0.00084	43			
1983	0.85 ± 0.023	0.019 ± 0.00084	43			
1985	0.89 ± 0.023	0.020 ± 0.00098	50			
1990	0.88 ± 0.023	0.019 ± 0.00087	44			
1992	0.90 ± 0.024	0.020 ± 0.00089	44			
1994	1.1 ± 0.023	0.028 ± 0.0011	62			
1998	1.3 ± 0.025	0.035 ± 0.0013	70			
2000	1.3 ± 0.025	0.035 ± 0.0013	70	2000-2012	509 ± 7	42 ± 0.6
2004	1.9 ± 0.035	0.062 ± 0.0019	79			
2008	2.6 ± 0.042	0.10 ± 0.0026	112			
2010	2.8 ±0.046	0.11 ± 0.0028	119			
2012	3.0 ± 0.047	0.12 ± 0.0030	120	2012-2014	163 ± 4	81 ± 2
2016	3.5 ± 0.049	0.18 ± 0.0035	128	2014-2017	72 ± 4	24 ± 1
2018	3.5 ± 0.050	0.17 ± 0.0035	126	2017-2019	31 ± 4	15 ± 2
2021	3.7 ± 0.050	0.19 ± 0.0036	128	2019-2021	21 ± 4	11 ± 2
2030	4.7 ± 0.92	0.26 ± 0.087	128	2021-2030	342 ± 5	38 ± 0.5
2040	5.7 ± 0.85	0.34 ± 0.11	146	2030-2040	380 ± 5	38 ± 0.5
2050	6.7 ± 0.87	0.42 ± 0.13	207	2040-2050	380 ± 5	38 ± 0.5
2060	7.5 ± 0.86	0.50 ± 0.14	210	2050-2060	380 ± 5	38 ± 0.5
2070	8.2 ± 1.0	0.54 ± 0.16	210	2060-2070	380 ± 5	38 ± 0.5
2080	8.5 ± 1.0	0.57 ± 0.16	210	2070-2080	380 ± 5	38 ± 0.5
2090	8.8 ± 1.1	0.59 ± 0.17	210	2080-2090	380 ± 5	38 ± 0.5
2100	9.2 ± 1.2	0.62 ± 0.17	210	2090-2100	380 ± 5	38 ± 0.5
2110	9.7 ± 1.5	0.64 ± 0.18	210	2100-2110	380 ± 5	38 ± 0.5
2120	9.7 ± 1.5	0.64 ± 0.18	210	2110-2120	380 ± 5	38 ± 0.5
Uncertainty estimation methodology	[a] **Lake surface area and volume:** differences between surface areas and volumes calculated for lake surface elevations at intervals corresponding to dataset vertical uncertainties. 1945–2021: lake surface elevations of 4 m and 5 m (sonar scanner bathymetry and lidar datasets have vertical uncertainties of ± < 0.5 m). 2030–2120: lake surface elevations of -15 m and 5 m (radio-echo sounding dataset has vertical uncertainty of ± 20 m). [b] **Lake depth:** uncertainty for 1945–2021 is ± < 0.5 m (vertical uncertainty for sonar scanner bathymetry dataset); uncertainty for 2030–2120 is ± 20 m (vertical uncertainty for radio-echo sounding dataset). [c] **Total glacier terminus retreat:** extrapolated from horizontal uncertainties of glacier terminus positions for ~1890 (20 m); 1945 (10 m); 1982 (10 m); 2002 (5 m); and 2010 (2 m) (Hannesdóttir et al., 2020) by adding uncertainties of years within (or closest to) the time interval. [d] **Average annual glacier terminus retreat rate:** Uncertainty for total glacier terminus retreat rate averaged annually over time interval.					

230   **Table 1. Past (white shading) and projected future (green shading) evolution of Fjallsárlón and Fjallsjökull, showing lake surface area, volume, and maximum depth (below lake surface elevation of 5 m a.s.l.) at 20 time steps from 1945–2021; terminus retreat distance and average rate during nine time intervals from 1890–2021; and projected lake and glacier changes at decadal intervals from 2030–2120 (assuming continuation of 2000–2021 average annual terminus retreat rate of 38 m a⁻¹ and 2020 lake surface elevation of 5 m a.s.l.).**

4.4. Future lake and glacier evolution

235   Assuming the lake will continue to expand westwards and maintain its 2020 surface elevation, a future lake will cover a maximum of 9.7 ± 1.5 km^2 and contain up to 0.64 ± 0.18 km^3 of water (Table 1; Fig. 6). This is quite similar to estimates of 9.8 km^2 surface area and 0.65 km^3 volume based on radio-echo sounding data (Magnússon et al., 2012). This estimated lake will fill both overdeepened troughs, with maximum depth almost doubling from 128 m to 210 m (Table 1; Fig. 5). Though there are small areas ~5 m a.s.l. near the northern and southern lake shorelines, the rest of the basin is surrounded by higher-

240 elevation terrain and up to 30 m-high moraines, so the lake will likely only expand westward towards the retreating glacier terminus. Uncertainties were estimated by calculating surface areas and volumes for lake surface elevations of -15 m and 5 m (an interval that capt   ertical uncertainties of $\pm$ 20 m for radio-echo sounding datasets). Assuming that terminus retreat continues into the future at the average 2000–2021 rate of 38 m a^{-1} and occurs at a uniform pace across the glacier front (as a simple straight line across the terminus), Fjallsjökull's terminus will become partially land-based after 2070. The lake-

245 terminating section will progressively narrow as the lake expands into the northern overdeepening, with the glacier completely withdrawing from the lake around 2110 (Fig. 5).

4.5. Mass movement potential and glacial lake outburst flood threat

     Three sections of the valley walls   Fjallsjökull have slope angles >30° with vertical relief >200 m, giving them a high topographic potential to source mass movements. These zones are located on slopes beneath the peaks of

250 Miðaftanstindur and Eyðnatindur (part of Breiðamerkurfjall) and Ærfjallshöfuð (part of Ærfjall) (Fig. 7). Though the valley walls have not been comprehensively geologically or structurally mapped, remote sensing and field observations reveal that they are primarily composed of rock with little or no overlying soil or sediment. No evidence of previous mass movements appears on Fjallsjökull in aerial photos (Landmælingar Íslands, 2022; Loftmyndir ehf., 2022).
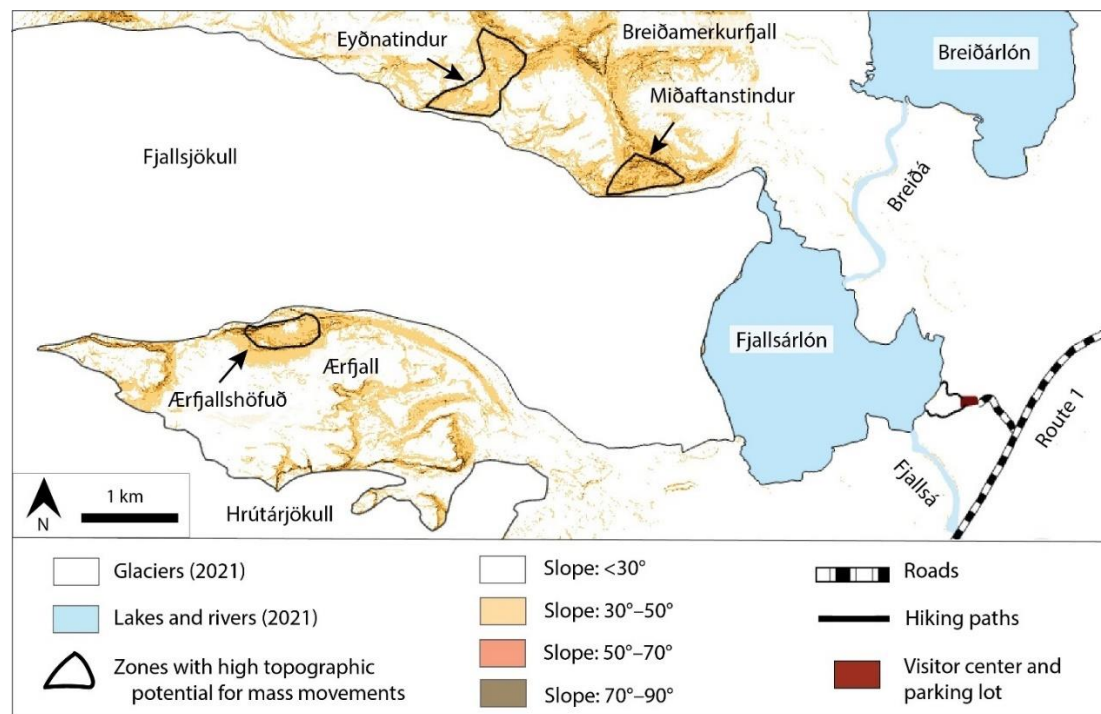
Figure 7. Map of slope angles on subaerial terrain in study area. Delineated zones show areas in valley walls above Fjallsjökull with slope angles >30° and vertical relief >200 m, indicating high topographic potential to source mass movements. ÍslandsDEM basemap with slope shading in ArcGIS Pro (Landmælingar Íslands, 2021).

Miðaftanstindur, Eyðnatindur, and Ærfjallshöfuð are 1100 m, 3200 m, and 4500 m, respectively, from the 2021 glacier terminus, so a mass movement event would travel across the glacier surface to reach the lake (Table 2). However, if Fjallsárlón evolves according to the estimated timeline (based on annual average terminus retreat rates of 38 m a^{-1}), Miðaftanstindur will be situated directly above the lake beginning around 2050 (Fig. 5). After the lake reaches its estimated maximum extent around 2110, a mass movement event from Eyðnatindur would travel 400 m to reach the shoreline, while one from Ærfjallshöfuð would travel 1700 m to the lakeshore (Table 2). Maximum vertical fall height for mass movement events from the three zones will increase as Fjallsjökull retreats. The highest point on Miðaftanstindur is 490 m above the 2021 glacier surface, an elevation that will increase to 600 m above the future lake surface. Maximum vertical fall heights for Eyðnatindur and Ærfjallshöfuð will increase from 520 m and 370 m above the 2021 glacier surface to 800 m and 870 m above the future lake surface, respectively. For a mass movement that enters the lake, the H/L ratio and angle of reach are highest for Miðaftanstindur, followed by Eyðnatindur and Ærfjallshöfuð, and will increase in each zone as the glacier retreats and the lake expands. The H/L ratios range from 0.18–1.2, while angles of reach are between 10° and 50° (Table 2).

Topographic parameter		Zone		
		Miðaftanstindur	Eyðnatindur	Ærfjallshöfuð
2021 glacier and lake positions	Maximum vertical height above glacier surface (m)	490	520	370
	Horizontal distance from zone to glacier terminus (m)	1100	3200	4500
	H/L ratio from zone to glacier terminus	H = 600 L = 1600 H/L = 0.38	H = 800 L = 4100 H/L = 0.20	H = 870 L = 4900 H/L = 0.18
	Angle of reach (fahrböschung) for H/L ratio from zone to glacier terminus (°)	21°	11°	10°
	Horizontal distance between highest and lowest zone boundaries (m)	500	900	400
Estimated future glacier and lake positions in ~2120	Maximum vertical height above estimated future lake surface (m)	600	800	870
	Horizontal distance from zone to lakeshore (m)	0	400	1700
	H/L ratio from zone to lakeshore	H = 600 L = 500 H/L = 1.2	H = 800 L = 1300 H/L = 0.62	H = 870 L = 2100 H/L = 0.41
	Angle of reach (fahrböschung) for H/L ratio from zone to lakeshore (°)	50°	32°	22°

Table 2. Topographic parameters to assess potential for mass movements to enter Fjallsárlón from the three identified zones for 2021 glacier and lake positions (white shading) and estimated glacier and lake positions in ~2120 when Fjallsjökull is projected to have retreated completely from the lake (green shading).

5. Discussion

5.1. Lake bathymetry, volume, and evolution

The multibeam sonar survey provided a higher-resolution dataset for the bed DEM than was previously reported for Fjallsárlón from radio-echo sounding surveys and weighted rope point measurements, though volume differences between methods were within calculated uncertainties. This more detailed bathymetric map can be used for future studies on glacial erosional processes (i.e. overdeepening formation), depositional features (i.e. identifying subaqueous landforms), and the role of bathymetry in lake–terminus interactions (i.e. calving processes) (Purdie et al., 2016; Minowa et al., 2023).

Given the challenge of surveying glacial lakes in often remote and mountainous environments (Peng, 2023; Ramsankaran et al., 2023), many lake volumes are estimated with models based on ice thickness and proglacial and subglacial topography (Carrivick et al., 2022; Colonia et al., 2017; Frey et al., 2010; Grab et al., 2021; Linsbauer et al., 2016; Magnin et al., 2020; Otto et al., 2022). Other studies have developed empirical equations that use lake surface area to estimate volume (Huggel et al., 2002; Loriaux and Cassassa, 2013; Cook and Quincey, 2015). However, both models and equations are highly

uncertain in estimating volume, especially in overdeepened basins (Cook and Quincey, 2015; Mölg et al., 2021; Kapitsa et al., 2023). Our bathymetric data offered an opportunity to test sonar scanner-derived volumes with a selection of empirical equations developed from lakes with similar sizes as Fjallsárlón (Table 3). Percent error between sonar scanner-derived volume and equation-predicted values varied from -13 to 16%, indicating fairly good agreement. However, this uncertainty also supports conclusions that equations do not accurately represent all glacial lake settings—particularly lakes such as Fjallsárlón that are in overdeepened basins and are not moraine- or ice-dammed. This illustrates the importance of directly measuring bathymetry to calculate volume and the need for more field-based datasets from overdeepened basins.

Study	Equation (V = volume; A = surface area)	Calculated volume (km³)	Percent error (%) (defined as: ((calculated volume–measured volume)/(measured volume)) * 100)
This study	Measured volume (from sonar scanner survey)	0.19	N/A
Cook and Quincey (2015)	$V = 0.1746 * A^{1.3725}$	0.18	-4.7
Huggel et al. (2002)	$V = 0.104 * A^{1.42}$	0.22	16
Loriaux and Casassa (2013)	$V = 0.2933 * A^{1.3324}$	0.16	-13

Table 3. Comparison of Fjallsárlón volume measured from sonar scanner survey with lake volumes predicted by selected empirical equations developed from lakes with similar sizes as Fjallsárlón.

One source of uncertainty in past and future lake volume calculations is how much sediment infill occurs since sonar scanner surveys map the lake floor, not necessarily bedrock. Sediment thickness and sedimentation rate in Fjallsárlón are unknown and would require coring to determine, and they may have changed over time, adding uncertainty to calculated lake volumes. Sediment influx could also increase under future climate warming due to greater subglacial meltwater runoff and erosion and/or supraglacial material sourced from mass movement events onto the glacier surface (Schomacker, 2010; Carrivick and Tweed, 2021; Ballantyne, 2022). Increased sediment input can decrease basin volume and thus lake storage capacity, so future lake volume estimates should be considered as maximum values (Magnin et al., 2020; Emmer et al., 2022; Steffen et al., 2022; Hosmann et al., 2024). Another unknown factor in future lake volume estimates is surface elevation of the Fjallsá river outlet (Purdie et al., 2016). However, Fjallsá base level is controlled by sea level, which is only 5 m below the current lake surface elevation—so while lake outlet geometry could lower via incision, this 5 m difference is captured in the uncertainty range of future volume estimates.

5.2. Future glacier evolution and lake–terminus interactions

Many factors contribute to glacier retreat and advance rates, including climate, ice velocity, subglacial topography, and lake–terminus interactions (Aðalgeirsdóttir et al., 2011; Cook and Swift, 2012; Dell et al., 2019; Jóhannesson et al., 2020). Thus, future glacier terminus evolution should be considered as a first order estimate. Numerous studies have projected future evolution of glaciers in Iceland, though results vary significantly depending on model spatial scale (global, Iceland, or ice cap),

emission scenarios, and type of ice flow model. Nonetheless, all models project at least an 18% volume loss for Vatnajökull by 2100 (Schmidt et al., 2020; Compagno et al., 2021; Rounce et al., 2023). In addition to climate scenarios and consequent surface mass balance, future glacier evolution is also controlled by meltwater runoff, subglacial water infiltration, calving,

315 lake-induced melting at the terminus, and subglacial geothermal melting—which are not all captured in every model (Jóhannesson et al., 2020; Schmidt et al., 2020). Given this complexity, projecting volume change and retreat rate for Fjallsjökull specifically will require modelling at the individual outlet glacier scale. This has previously been done for another Vatnajökull outlet glacier, Hoffellsjökull, indicating a ~30% volume loss by 2100 (relative to its 2010 volume) if average climate conditions from 2000–2009 continue, with the glacier nearly disappearing by 2100 under projected temperature

320 increases of 1°–3°C (Aðalgeirsdóttir et al., 2011). However, usual simplifications in dynamic ice flow models are not suited for the complex topography of Fjallsjökull due to its narrow outlet, steeply sloping bed, and relatively thin, highly crevassed ice flow over undulated bedrock.

Another uncertainty in future glacier and lake evolution is lake–terminus interactions. When Fjallsjökull enters the northern overdeepened trough, maximum lake depth will nearly double from its deepest point in 2021. This will increase the

325 surface area at the glacier front that is in contact with lake water, increasing melt. Deeper water will also increase torque and buoyancy forces at the terminus and thus calving rates. This, in turn, may reduce effective pressure and longitudinal stress, increasing ice flow and resulting in glacier thinning (Motyka et al., 2002; Benn et al., 2007; Dell et al., 2019; Baurley et al., 2020; Carrivick et al., 2020; Sutherland et al., 2020; Minowa et al., 2023). Increased lake depth and buoyancy force could also float the glacier tongue, eliminating basal friction at the glacial bed and increasing ice flow velocity and thus thinning,

330 crevassing, and ice disintegration (Motyka et al., 2002; Benn et al., 2007; Boyce et al., 2007; Baurley et al., 2020; Main et al., 2022). Terminus flotation has occurred at Heinabergsjökull and Hoffellsjökull, other Vatnajökull outlet glaciers (Aðalgeirsdóttir et al., 2011; Guðmundsson et al., 2019).

Even if calving rates increase, the lake-terminating glacier front will become narrower as Fjallsjökull retreats into the northern overdeepening, potentially reducing the amount of mass loss through calving (Fig. 5). In 2021, the terminus calving

335 front was 2.7 km wide. Assuming the glacier and lake evolve at the estimated rates, the calving front will span ~2 km around 2050 and ~1 km around 2080. Moreover, retreat rates will likely vary across the terminus, resulting in different configurations than the estimated simple straight line shapes (Fig. 5). Part of the terminus is projected to become land-based around 2070, which may retreat at a different rate than the lake-terminating front; though our calculated average annual 2000–2021 retreat rate includes both lake- and land-terminating sections, which may capture these differences.

340 5.3. Mass movement scenarios into Fjallsárlón

Though three zones of the valley walls above Fjallsjökull have a high topographic potential of sourcing mass movements, we cannot predict the exact location, volume, or failure plane of an event without comprehensive geological and structural mapping (McColl, 2012; Hartmeyer et al., 2020). However, several scenarios are possible for mass movements to enter Fjallsárlón and generate displacement waves or GLOFs (Fig. 8). Given the predominant rock composition of the valley

345 walls, a mass movement event will likely be a rock slope failure such as a rock fall (with a volume lower than the threshold
for material to flow, causing most material to be deposited near the failure slope) or rock avalanche (with a volume exceeding
the threshold for flow, enabling material to travel away from the source area), with the classification determined by the vertical
fall height (H), horizontal travel distance (L), and angle of reach (Evans et al., 2006; Hungr et al., 2014; Hermanns et al., 2022).
At the estimated future maximum lake extent, the H/L ratio and angle of reach at Miðaftanstindur will exceed the thresholds

350 of 0.625 and 32°, respectively, meaning that a rock fall would enter the lake. For all other scenarios (from all three zones in
2021 and Eyðnatindur and Ærfjallshöfuð at future maximum lake extent), H/L ratios are <0.625 and angles of reach are ≤32°,
so mass movements must have large enough volumes to classify as rock avalanches in order to reach the lake.
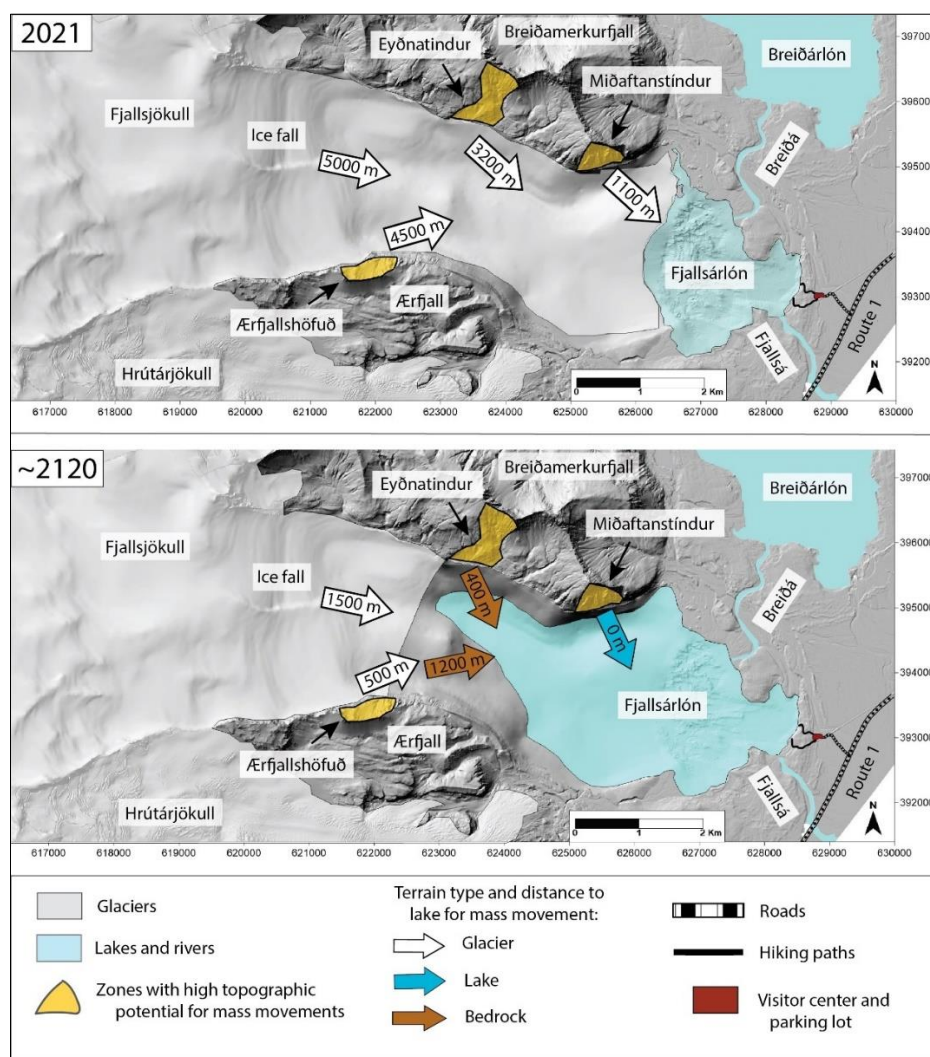
Figure 8. Scenarios of mass movements entering Fjallsárlón based on glacier and lake positions in 2021 and estimated glacier and
355 **lake extents in ~2120 when Fjallsjökull is projected to have retreated completely from the lake. Bed DEM basemap.**

Several factors control mass movement mobility and runout distance and thus whether material will reach Fjallsárlón. Material traveling across a glacier will have high mobility due to low friction on the glacier surface and frictional melting of ice, resulting in a greater runout distance (Sosio et al., 2012; De Blasio, 2014; Deline et al., 2022). Fjallsjökull's surface gradient in 2021 was approximately 6° along the central flow line for the section down-valley of the three identified zones.

360 There are numerous global precedents of rock avalanches onto glaciers with similar gradients and angles of reach where runout distances have exceeded 4500 m, the longest horizontal distance in our scenarios (Sosio et al., 2012; Delaney and Evans, 2014; Sosio, 2015; Aaron and McDougall, 2019; Ben-Yehoshua et al., 2022; Deline et al., 2022). Increased water content can also increase rock fall or rock avalanche mobility and thus runout distance. If a failure plane extends from the valley wall under the glacier, a mass movement event could fracture the glacier and incorporate glacial ice, increasing mobility by reducing friction

365 between clasts and adding meltwater to the material (Sosio et al., 2012; Deline et al., 2022). Additionally, the large maximum vertical fall heights at all three zones mean that a rock fall or rock avalanche may transfer enough energy to fracture or melt the glacier, incorporating ice blocks and water (Byers et al., 2019; Shugar et al., 2021). Vertical fall heights (and thus potential energy transfer) will increase with projected glacier thinning—though this mass loss will also reduce the ice volume available to fracture or melt. Given these potential interactions with the glacier, it is possible that a rock fall onto Fjallsjökull could

370 become mobile enough to transform into a rock avalanche and travel down the glacier to enter the lake.

Out of all scenarios, a mass movement from Miðaftanstindur after ~2070 may pose the greatest GLOF threat since the lake will have expanded beneath the entire mountain by this time, resulting in direct energy transfer to the lake rather than attenuation during impact and travel across the glacier. For all other scenarios, GLOF threat will also likely increase with future projected Fjallsjökull terminus retreat. With all other factors remaining equal, decreased horizontal travel distances

375 between high topographic potential zones and the lake indicate that: 1) a rock avalanche with a smaller volume will be able to reach the lake; and 2) a rock avalanche will lose less energy along its shorter travel path and transfer more material to the lake to generate larger displacement waves. However, terrain type along the rock avalanche travel path will also change as the terminus retreats, potentially reducing this increased GLOF threat. At the estimated maximum lake extent around 2110, a rock avalanche from Eyðnatindur will travel across 400 m of bedrock terrain to reach the lake, while one from Ærfjallshöfuð will

380 travel 500 m across the glacier surface and 1200 m across bedrock terrain (Fig. 8). This bedrock terrain will increase surface friction and eliminate interactions with ice, reducing material mobility and runout distance. Finally, it is important to note that while three identified zones have high topographic potential of sourcing mass movements, slope failures could occur from other locations in the valley walls due to structural weaknesses such as faults or fractures or a high degree of weathering. Moreover, GLOF threat from Fjallsárlón will likely persist after Fjallsjökull retreats from the lake basin around 2110 since

385 glacial meltwater will continue to drain into the lake, and valley walls will continue to experience paraglacial instability.

A mass movement from the valley walls above Fjallsjökull could be triggered by numerous processes. First, Fjallsjökull is an outlet glacier of Öræfajökull, which is an active volcano that experiences periodic seismic activity that could potentially generate a rock slope failure (Keefer, 1984; Einarsson, 2019). Second, extreme precipitation events could trigger rock slope failures by increasing pore water pressure and adding weight to slopes (Chigira, 2009; Chigira et al., 2013). This

390 process triggered a landslide in 2013 onto Svínafellsjökull, another Öræfajökull outlet glacier, that traveled nearly 4 km down the glacier surface (Ben-Yehoshua et al., 2022). Third, continued glacier retreat and thinning will expose new valley wall sections to paraglacial processes such as debuttressing, freeze-thaw activity, and crustal rebound stress adjustments, which could destabilize rock and result in rock falls or rock avalanches. However, one common paraglacial trigger of mass movements in other environments that is likely not a factor at Fjallsjökull is permafrost thaw. Estimated permafrost distribution

395 in Iceland is mostly in the northern and central highland regions and above 800–1000 m a.s.l. (Etzelmüller et al., 2007, 2020; Czekirda et al., 2019). Back-calculated ground temperatures on valley walls above Svínafellsjökull, which has a similar climatic setting to Fjallsjökull, indicate that permafrost conditions have not occurred below 1000 m a.s.l. since ~1900 (Ben-Yehoshua et al., 2022).

     Ice avalanches may also pose a threat of triggering a GLOF at Fjallsárlón, as they do at   glacial lakes worldwide

400 (Frey et al., 2010; Schaub et al., 2016; Tang et al., 2023). Ice avalanches can fall from overhanging valley glaciers or result from changes in glacier dynamics, such as ice velocity increases, deeper or more spatially extensive crevassing, or changes in glacier hydrology or geometry that alter ice masses and decrease basal friction at the bed (Evans and Clague, 1994; Deline et al., 2015). While there are no visible ice overhangs on the valley walls, an ice fall occurs ~5 km from the 2021 terminus where the glacier flows over bedrock steps—a distance that will shorten to ~1.5 km when the lake expands to its projected future

405 maximum extent around 2110 (Fig. 8). Glacier stress dynamics in this ice fall may change as atmospheric temperatures increase and the terminus enters deeper water. Additionally, large calving events from the glacier terminus may generate displacement waves in Fjallsárlón (Cook et al., 2016).

     Finally, even if a rock avalanche occurs from the slopes above Fjallsjökull and does not continue into the lake, it could influence future glacier dynamics by insulating the surface to slow melting (with thicker debris cover), increasing

410 ablation to enhance melting (with thinner debris cover), changing glacier velocity or sediment transport, or depositing material on the glacier surface for mobilization by another rock avalanche (Haritashya et al., 2018; Bessette-Kirton and Coe, 2020; Deline et al., 2022). Thus, projecting the location and dynamics of potential mass movements onto Fjallsjökull is important even if they do not enter Fjallsárlón.

5.4. Glacial lake outburst flood threat and potential impacts

415   Even if a rock fall, rock avalanche, or ice avalanche enters Fjallsárlón, it will not necessarily generate a displacement wave, and it will only trigger a GLOF downstream if waves exit the lake basin. Displacement wave propagation dynamics and runup height depend on mass movement velocity, volume, geometry, and lake entry angle; lake bathymetry and shoreline geometry; and whether the wave travels as a single wave or seiche wave (repeated waves in the basin) (Romstad et al., 2009; Westoby et al., 2014a; Oppikofer et al., 2018). Given the current level of knowledge, we cannot accurately predict displacement

420 wave behavior—only impacts of potential runup wave scenarios.

     Though Fjallsárlón is not moraine-dammed, moraines surround most of its shoreline. Displacement waves exceeding ~25 m high would overtop the tallest moraines, potentially continuing as a GLOF downstream. Waves could also incise the

moraines to create a lower-elevation breach for subsequent, smaller waves to exit (Hubbard et al., 2005; Evans et al., 2006; Emmer and Vilímek, 2013; Westoby et al., 2014a). Displacement waves of any height could exit the lake via the Fjallsá outlet,

425 which forms a topographic low point along the shoreline. If a mass movement enters Fjallsárlón, the greatest distance for displacement waves to travel between any points along the 2021 lake shoreline is ~2.5 km, which will increase to ~6 km at estimated future maximum lake extent around 2110. Mass movement-triggered displacement waves have exceeded 25 m high and traveled more than 6 km at lakes with similar sizes to Fjallsárlón, including in Iceland (Gylfadóttir et al., 2017) and Canada (Roberts et al., 2013), indicating that (though dependent on mass movement characteristics) waves could realistically exit the

430 Fjallsárlón basin and drain in a GLOF.

A displacement wave or GLOF at Fjallsárlón could have a significant societal impact. If overtopping or breaching occurs at the moraines on the eastern lakeshore, floodwaters could inundate a visitor center and parking lot approximately 300 m downstream, as well as hiking paths in between. A displacement wave with a runup height of even 1 m could impact people on the shoreline, which is a popular viewpoint and the launch site for boat tours on Fjallsárlón. If a wave surged through the

435 lake outlet to drain along the Fjallsá river, it would travel only ~1 km before reaching a bridge along Route 1 (Fig. 9). This is Iceland's main road and the only land transport and supply connection between east and west Iceland on the south coast, so damage to the road or bridge could have significant economic and tourism impacts not just at Fjallsjökull but at a regional scale (Welling et al., 2020; Welling and Abegg, 2021). Moreover, these infrastructure and visitor sites are concentrated on the eastern edge of the lake, which is roughly perpendicular to the direction from which a mass movement from any of the three

440 identified zones would enter Fjallsárlón, and displacement waves tend to be highest when they approach perpendicular to a location (Frey et al., 2018; Hermanns et al., 2022).

A GLOF from Fjallsárlón would also significantly impact the landscape. Based on Fjallsjökull's proglacial geomorphology and impacts observed in similar depositional settings, an outburst flood would likely erode channels in sediment (including enlarging the Fjallsá outlet), transport moraine and sandur material, and deposit boulders, gravel bars,

445 and/or sediment fans (Kershaw et al., 2005; Russell et al., 2006; Wilson et al., 2019; Chandler et al., 2020; Wells et al., 2022). This material redistribution could damage or destroy roads, trails, the bridge, the parking lot, and the tourist center, leaving a long-term geomorphologic legacy after floodwaters receded (Fig. 9).
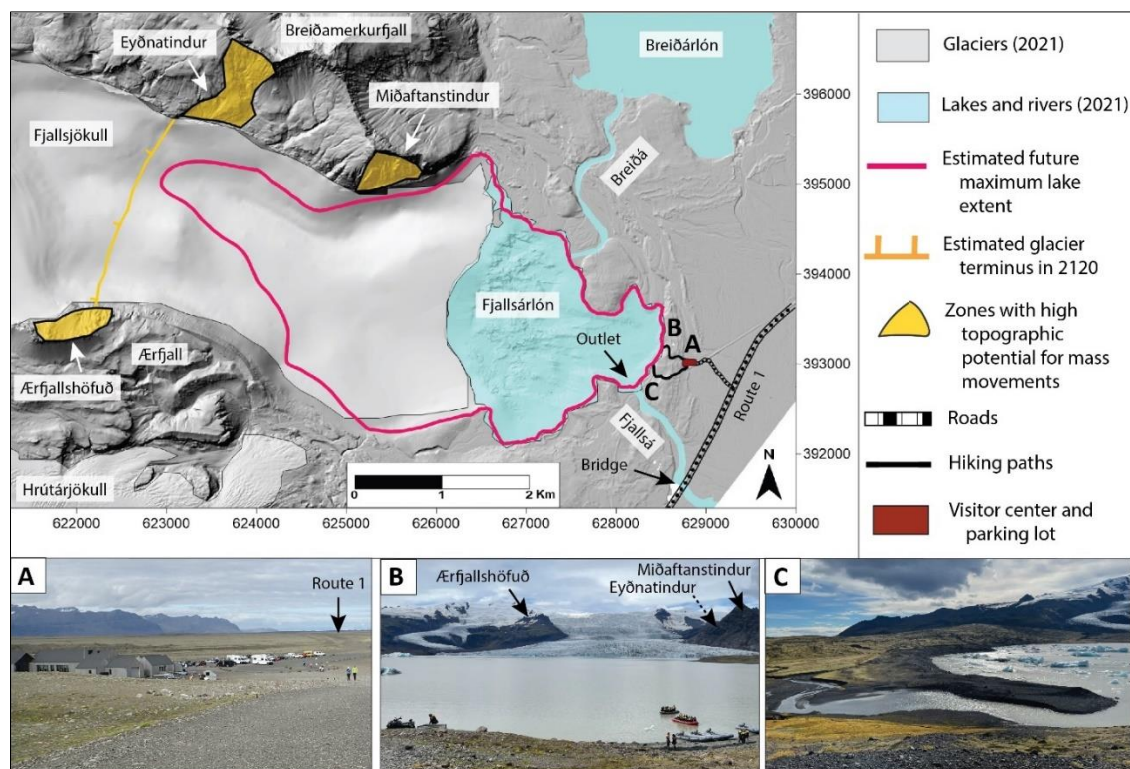
Figure 9. Map illustrating potential societal and landscape impacts of mass movement-triggered displacement waves and/or GLOFs in Fjallsárlón based on 2021 and estimated 2120 glacier and lake positions. Bed DEM basemap. Photos A–C correspond to locations marked on the map: (A) View looking northeast towards the visitor center, parking lot, and Route 1. (B) View looking west towards Fjallsjökull showing hiking trails and boat launches along the lakeshore, with high topographic potential zones marked. (C) View looking southwest across the proglacial landscape showing moraines and outwash sediments.

Though a comprehensive risk and hazard assessment is beyond the scope of this study, our results provide information that can contribute to developing one. Lake bathymetry and identification of potential mass movement source areas are crucial input datasets for modelling displacement wave propagation and dam breach scenarios (Harbitz et al., 2014; Worni et al., 2014; Haritashya et al., 2018; Lala et al., 2018; Mergili et al., 2020; Sattar et al., 2021; Rinzin et al., 2023). Additionally, lake extent, volume, and proglacial topography serve as inputs for numerical hydraulic modelling to simulate flood routes and dynamics, which can help predict geomorphologic impacts—for example, zones of erosion versus deposition and the type of material involved—to prepare for repair and clean-up efforts (Westoby et al., 2014b; Allen et al., 2022; Geertsema et al., 2022; Sattar et al., 2023). Finally, this study identifies three zones with high topographic potential of mass movements to prioritize for geological and structural mapping and monitoring, perhaps following approaches at unstable slopes at other locations (Purdie et al., 2015; Kos et al., 2016; Hartmeyer et al., 2020; Svennevig et al., 2020; Lacroix et al., 2022; Ben-Yehoshua et al., 2023; Moragues et al., 2024). Taken together, this research can help local and national authorities to develop risk assessments, plan future infrastructure and tourism access, and communicate this new, emerging hazard to locals and visitors (Stewart et al., 2016; Strzelecki and Jaskólski, 2020; Matti and Ögmundardóttir, 2021; Welling and Abegg, 2021; Matti et al., 2023).

6. Conclusions

Fjallsárlón has significantly expanded since it was first mapped in 1945, increasing in surface area by 3.4 km^2 and in volume by 0.18 km^3 to cover 3.7 ± 0.050 km^2 and contain 0.19 ± 0.0036 km^3 of water by 2021. Over the same time interval,
470 measured maximum water depth increased from 32 m to 128 m as the lake expanded into an overdeepened basin. Sonar scanner-derived lake volumes generally match those estimated from radio-echo sounding surveys and weighted rope point measurements, indicating good agreement between met   However, differences are greater when sonar scanner-derived volumes are compared with those calculated from empirical equations, calling for more field measurements to refine equations, especially from lakes in overdeepened basins.

475 If Fjallsárlón maintains its 2020 surface elevation, the lake will reach a maximum surface area of 9.7 ± 1.5 km^2 and volume of 0.64 ± 0.18 km^3, fill the rest of the southern overdeepened basin, and occupy the northern trough, increasing its maximum depth to ~210 m. Though Fjallsjökull's future behavior has not yet been modeled at an outlet glacier scale, regional-scale glacier evolution projections indicate that Vatnajökull will continue to lose mass under all emission scenarios (Schmidt et al., 2020; Compagno et al., 2021; Rounce et al., 2023). Assuming that terminus retreat continues at the 2000–2021 rate,
480 Fjallsjökull will retreat out of the lake basin around 2110, with sections of its terminus becoming land-based after ~2070. Glacier retreat into the northern overde   ng will likely increase ice loss due to greater calving rates and subaqueous melting, which—along with projected climate warming—will increase ice thinning and velocity and potentially cause flotation of the glacier tongue. However, numerous factors control future glacier and lake evolution; thus, projections made here should be considered as a first order estimate (though likely a minimum rate) rather than a realistic timeline for retreat.

485 Three zones on the valley walls above Fjallsjökull have a high topographic potential for sourcing mass movements due to slope angles >30° and vertical relief >200 m: the slopes beneath Miðaftanstindur, Eyðnatindur, and Ærfjallshöfuð. Based on 2021 lake extent, a rock avalanche from these zones would travel between ~1100 m and ~4500 m before entering Fjallsárlón, which is realistic given increased mobility from reduced friction of the ice surface and likely incorporation of meltwater. A mass movement from Miðaftanstindur poses the greatest threat of triggering a GLOF since it is situated closest
490 to Fjallsárlón, and a rock fall or rock avalanche after ~2050 could directly enter the lake. GLOF threat will also likely increase from Eyðnatindur and Ærfjallshöfuð as Fjallsjökull retreats, with rock avalanche travel distance to the lake decreasing to ~400 m and ~1700 m, respectively, at estimated maximum lake extent. However, material will flow over higher-friction bedrock terrain, potentially reducing runout distance.

If a rock fall, rock avalanche, or ice avalanche enters Fjallsárlón, displacement waves with runup heights as low as 1
495 m could impact visitors and boats on the shoreline. If runup heights exceed ~25 m, waves could overtop and/or incise the highest moraines on the lake's eastern shore, inundating the tourist center and parking lot ~300 m downstream. Displacement waves could also exit the lake through the Fjallsá river outlet and continue as a GLOF ~1 km to Route 1 road and bridge. These scenarios could significantly impact human security, infrastructure, and transportation connections, with societal and economic

effects extending throughout the region. A GLOF would also erode and redistribute large quantities of sediment and moraine material, leaving a long-term geomorphologic legacy.

Mass movement-triggered GLOFs will likely pose a greater threat at other proglacial lakes in Iceland and Arctic and alpine regions worldwide as climate warming continues. Measuring lake bathymetry, quantifying past lake change, and projecting future lake evolution are crucial for understanding how glaciers, hydrology, and landscapes respond to climate change. This is especially important in regions like southern Vatnajökull where visitor numbers and infrastructure development are increasing, and future planning should assess risk from these emerging hazards to mitigate societal impact. Results from Fjallsárlón can inform studies at similar sites in Iceland, as well as other glaciated regions across the globe.

Author contribution

GHW prepared the manuscript with review and editing by all co-authors. GHW and ÞS conceptualized the project. FP and EM provided radio-echo sounding data. ÞS collected sonar scanner bathymetric data. SG provided glacial lake outlines from 1945–2018.

Competing interests

The authors declare that they have no conflict of interest.

Acknowledgements

This project was completed as part of a University of Iceland Post-doc Grant to GHW. The multibeam sonar scanner bathymetric survey of Fjallsárlón in 2020 was conducted by Köfunarþjónustan and funded by a grant to ÞS from the Landsvirkjun Energy Research Fund (Orkurannsóknasjóður Landsvirkjunar, received in 2019).

References

Aaron, J. and McDougall, S.: Rock avalanche mobility: The role of path material, Eng. Geol., 257, 105126, https://doi.org/10.1016/j.enggeo.2019.05.003, 2019.

Aðalgeirsdóttir, G., Guðmundsson, S., Björnsson, H., Pálsson, F., Jóhannesson, T., Hannesdóttir, H., Sigurðsson, S.P., and Berthier, E.: Modelling the 20th and 21st century evolution of Hoffellsjökull glacier, SE-Vatnajökull, Iceland, Cryosphere, 5, 961–975, https://doi.org/10.5194/tc-5-961-2011, 2011.

Aðalgeirsdóttir, G., Magnússon, E., Pálsson, F., Thorsteinsson, T., Belart, J.M.C., Jóhannesson, T., Hannesdóttir, H., Sigurðsson, O., Gunnarsson, A., Einarsson, B., Berthier, E., Schmidt, L.S., Haraldsson, H.H., and Björnsson, H., Glacier changes in Iceland from ~1890 to 2019, Front. Earth Sci., 8, 574754, https://doi.org/10.3389/feart.2020.523646, 2020.

Allen, S.K., Zhang, G., Wang, W., Yao, T., and Bolch, T.: Potentially dangerous glacial lakes across the Tibetan Plateau

530   revealed using a large-scale automated assessment approach, Sci. Bull., 64, 435–445,
         https://doi.org/10.1016/j.scib.2019.03.011, 2019.

Allen, S.K., Sattar, A., King, O., Zhang, G., Bhattacharya, A., Yao, T., and Bolch, T.: Glacial lake outburst flood hazard under
         current and future conditions: Worst-case scenarios in a transboundary Himalayan basin, Nat. Hazards Earth Syst.
535   Sci., 22, 3765–3785, https://doi.org/10.5194/nhess-22-3765-2022, 2022.

Ballantyne, C.K.: Paraglacial geomorphology, in: Encyclopedia of Quaternary Science, 3rd ed., Elsevier, 1-22,
         https://doi.org/10.1016/b978-0-323-99931-1.00003-9, 2022.

540   Baurley, N.R., Robson, B.A., and Hart, J.K.: Long-term impact of the proglacial lake Jökulsárlón on the flow velocity and
         stability of Breiðamerkurjökull glacier, Iceland, Earth Surf. Proc. Land., 45, 2647-2663,
         https://doi.org/10.1002/esp.4920, 2020.

Belart, J.M.C. and Magnússon, E.: Pléiades data as part of the CEOS Geohazard Supersites,
545   https://ceos.org/ourwork/workinggroups/disasters/gsnl/, 2024.

Belart, J.M.C., Magnússon, E., Berthier, E., Gunnlaugsson, Á.Þ., Pálsson, F., Aðalgeirsdóttir, G., Jóhannesson, T.,
         Thorsteinsson, T., and Björnsson, H.: Mass balance of 14 Icelandic glaciers, 1945–2017: Spatial variations and links
         with climate, Front. Earth Sci., 8, 163, https://doi.org/10.3389/feart.2020.00163, 2020.
550
Ben-Yehoshua, D., Sæmundsson, Þ., Helgason, J.K., Belart, J.M.C., Sigurðsson, J.V., and Erlingsson, S.: Paraglacial exposure
         and collapse of glacial sediment: The 2013 landslide onto Svínafellsjökull, southeast Iceland, Earth Surf. Proc. Land.,
         47, 2612–2627, https://doi.org/10.1002/esp.5398, 2022.

Ben-Yehoshua, D., Sæmundsson, Þ., Helgason, J.K., Hermanns, R.L., Magnússon, E., Ófeigsson, B.G., Belart, J.M.C.,
555   Hjartardóttir, Á.R., Geirsson, H., Gu, S., and Hannesdóttir, H.: The destabilization of a large mountain slope
         controlled by thinning of Svínafellsjökull glacier, SE Iceland, Jökull, 73, 1–33,
         https://doi.org/10.33799/jokull2023.73.001, 2023.

Benn, D.I., Warren, C.R., and Mottram, R.H.: Calving processes and the dynamics of calving glaciers. Earth-Sci. Rev., 82,
         143–179, https://doi.org/10.1016/j.earscirev.2007.02.002, 2007.
560
Bessette-Kirton, E.K. and Coe, J.A.: A 36-year record of rock avalanches in the Saint Elias Mountains of Alaska, with
         implications for future hazards, Front. Earth Sci., 8, 293, https://doi.org/10.3389/feart.2020.00293, 2020.

Björnsson, H.: Subglacial lakes and jökulhlaups in Iceland, Global Planet. Change, 35, 255–271,
565   https://doi.org/10.1016/S0921-8181(02)00130-3, 2002.

Björnsson, H., Pálsson, F., Gudmundsson, S., Magnússon, E., Adalgeirsdóttir, G., Jóhannesson, T., Berthier, E., Sigurdsson,
         O., and Thorsteinsson, T.: Contribution of Icelandic ice caps to sea level rise: Trends and variability since the Little
         Ice Age, Geophys. Res. Lett., 40, 1546–1550, https://doi.org/10.1002/grl.50278, 2013.
570
Böhme, M., Morken, O. A., Oppikofer, T., Hermanns, R. L., Penna, I., Nicolet, P., Bredal, M., Pullarello, J., and Noël,
         F.: Towards a national susceptibility map for rock avalanches, EGU General Assembly 2022, Vienna, Austria, 23–
         27 May 2022, EGU22-12124, https://doi.org/10.5194/egusphere-egu22-12124, 2022.

Boyce, E.S., Motyka, R.J., and Truffer, M.: Flotation and retreat of a lake-calving terminus, Mendenhall Glacier, southeast
575   Alaska, USA, J. Glaciol., 53, 211–224, https://doi.org/10.3189/172756507782202928, 2007.

Bradwell, T.: Lichenometric dating in southeast Iceland: The size-frequency approach, Geogr. Ann. A., 86, 31–41, https://doi.org/10.1111/j.0435-3676.2004.00211.x, 2004.

580   Byers, A.C., Rounce, D.R., Shugar, D.H., Lala, J.M., Byers, E.A., and Regmi, D.: A rockfall-induced glacial lake outburst flood, Upper Barun Valley, Nepal, Landslides, 16, 533-549, https://doi.org/10.1007/s10346-018-1079-9, 2019.

Carrivick, J.L. and Tweed, F.S.: Proglacial lakes: Character, behaviour and geological importance, Quaternary Sci. Rev., 78, 34–52, https://doi.org/10.1016/j.quascirev.2013.07.028, 2013.

585   Carrivick, J.L. and Tweed, F.S.: A global assessment of the societal impacts of glacier outburst floods, Global Planet. Change, 144, 1–16, https://doi.org/10.1016/j.gloplacha.2016.07.001, 2016.

Carrivick, J.L. and Tweed, F.S.: A review of glacier outburst floods in Iceland and Greenland with a megafloods perspective. Earth-Sci. Rev., 196, 102876, https://doi.org/10.1016/j.earscirev.2019.102876, 2019.

590   Carrivick, J.L. and Tweed, F.S.: Deglaciation controls on sediment yield: Towards capturing spatio-temporal variability, Earth-Sci. Rev., 221, 103809, https://doi.org/10.1016/j.earscirev.2021.103809, 2021.

Carrivick, J.L., Tweed, F.S., Sutherland, J.L., and Mallalieu, J.: Toward numerical modeling of interactions between ice-
595   marginal proglacial lakes and glaciers, Front. Earth Sci., 8, 577068, https://doi.org/10.3389/feart.2020.577068, 2020.

Carrivick, J.L., Sutherland, J.L., Huss, M., Purdie, H., Stringer, C.D., Grimes, M., James, W.H.M., and Lorrey, A.M.: Coincident evolution of glaciers and ice-marginal proglacial lakes across the Southern Alps, New Zealand: Past, present and future, Global Planet. Change, 211, 103792, https://doi.org/10.1016/j.gloplacha.2022.103792, 2022.

600
Chandler, B.M.P., Evans, D.J.A., Chandler, S.J.P., Ewertowski, M.W., Lovell, H., Roberts, D.H., Schaefer, M., and Tomczyk, A.M.: The glacial landsystem of Fjallsjökull, Iceland: Spatial and temporal evolution of process-form regimes at an active temperate glacier, Geomorphology, 361, 107192, https://doi.org/10.1016/j.geomorph.2020.107192, 2020.

Chigira, M.: September 2005 rain-induced catastrophic rockslides on slopes affected by deep-seated gravitational
605   deformations, Kyushu, southern Japan, Eng. Geol., 108, 1–15, https://doi.org/10.1016/j.enggeo.2009.03.005, 2009.

Chigira, M., Tsou, C.-Y., Matsushi, Y., Hiraishi, N., and Matsuzawa, M.: Topographic precursors and geological structures of deep-seated catastrophic landslides caused by Typhoon Talas, Geomorphology, 201, 479–493, https://doi.org/10.1016/j.geomorph.2013.07.020, 2013.

Clague, J.J. and Evans, S.G.: A review of catastrophic drainage of moraine-dammed lakes in British Columbia, Quaternary
610   Sci. Rev., 19, 1763–1783, https://doi.org/10.1016/s0277-3791(00)00090-1, 2000.

Colonia, D., Torres, J., Haeberli, W., Schauwecker, S., Braendle, E., Giraldez, C., and Cochachin, A.: Compiling an inventory of glacier-bed overdeepenings and potential new lakes in de-glaciating areas of the Peruvian Andes: Approach, first results, and perspectives for adaptation to climate change, Water, 9, 336, https://doi.org/10.3390/w9050336, 2017.

615
Compagno, L., Zekollari, H., Huss, M., and Farinotti, D.: Limited impact of climate forcing products on future glacier evolution in Scandinavia and Iceland, J. Glaciol., 67, 727–743, https://doi.org/10.1017/jog.2021.24, 2021.

Cook, S.J. and Quincey, D.J.: Estimating the volume of Alpine glacial lakes, Earth Surf. Dynam., 3, 559–575,
620   https://doi.org/10.5194/esurf-3-559-2015, 2015.

Cook, S.J. and Swift, D.A.: Subglacial basins: Their origin and importance in glacial systems and landscapes, Earth-Sci. Rev., 115, 332–372, https://doi.org/10.1016/j.earscirev.2012.09.009, 2012.

Cook, S.J., Kougkoulos, I., Edwards, L.A., Dortch, J., and Hoffmann, D.: Glacier change and glacial lake outburst flood risk in the Bolivian Andes, Cryosphere, 10, 2399–2413, https://doi.org/10.5194/tc-10-2399-2016, 2016.

Czekirda, J., Westermann, S., Etzelmüller, B., and Jóhannesson, T.: Transient modelling of permafrost distribution in Iceland, Front. Earth Sci., 7, 130, https://doi.org/10.3389/feart.2019.00130, 2019.

De Blasio, F.V.: Friction and dynamics of rock avalanches travelling on glaciers, Geomorphology, 213, 88–98, https://doi.org/10.1016/j.geomorph.2014.01.001, 2014.

Delaney, K.B. and Evans, S.G.: The 1997 Mount Munday landslide (British Columbia) and the behaviour of rock avalanches on glacier surfaces, Landslides, 11, 1019–1036, https://doi.org/10.1007/s10346-013-0456-7, 2014.

Deline, P., Gruber, S., Delaloye, R., Fischer, L., Geertsema, M., Giardino, M., Hasler, A., Kirkbride, M., Krautblatter, M., Magnin, F., McColl, S., Ravanel, L., and Schoeneich, P.: Ice loss and slope stability in high-mountain regions, in: Snow and Ice-Related Hazards, Risks, and Disasters, edited by: Shroder, J.F., Haeberli, W., and Whiteman, C., Elsevier, 521–561, https://doi.org/10.1016/B978-0-12-394849-6.00015-9, 2015.

Deline, P., Hewitt, K., Shugar, D., and Reznichenko, N.: Rock avalanches onto glaciers, in: Landslide Hazards, Risks, and Disasters, 2nd ed., edited by: Davies, T., Rosser, N., and Shroder, J.F., Elsevier, 269-333, https://doi.org/10.1016/B978-0-12-818464-6.00010-X, 2022.

Dell, R., Carr, R., Phillips, E., and Russell, A.J.: Response of glacier flow and structure to proglacial lake development and climate at Fjallsjökull, south-east Iceland, J. Glaciol., 65, 321–336, https://doi.org/10.1017/jog.2019.18, 2019.

Dunning, S.A., Large, A.R.G., Russell, A.J., Roberts, M.J., Duller, R., Woodward, J., Mériaux, A.-S., Tweed, F.S., and Lim, M.: The role of multiple glacier outburst floods in proglacial landscape evolution: The 2010 Eyjafjallajökull eruption, Iceland, Geology, 41, 1123–1126, https://doi.org/10.1130/G34665.1, 2013.

Einarsson, P.: Historical accounts of pre-eruption seismicity of Katla, Hekla, Öræfajökull and other volcanoes in Iceland, Jökull, 69, 35–52, https://doi.org/10.33799/jokull2019.69.035, 2019.

Emmer, A.: Vanishing evidence? On the longevity of geomorphic GLOF diagnostic features in the Tropical Andes, Geomorphology, 422, 108552, https://doi.org/10.1016/j.geomorph.2022.108552, 2023.

Emmer, A. and Vilímek, V.: Review article: Lake and breach hazard assessment for moraine-dammed lakes: An example from the Cordillera Blanca (Peru), Nat. Hazards Earth Syst. Sci., 13, 1551–1565, https://doi.org/10.5194/nhess-13-1551-2013, 2013.

Emmer, A., Harrison, S., Mergili, M., Allen, S., Frey, H., and Huggel, C.: 70 years of lake evolution and glacial lake outburst floods in the Cordillera Blanca (Peru) and implications for the future, Geomorphology, 365, 107178, https://doi.org/10.1016/j.geomorph.2020.107178, 2020.

Emmer, A., Allen, S.K., Carey, M., Frey, H., Huggel, C., Korup, O., Mergili, M., Sattar, A., Veh, G., Chen, T.Y., Cook, S.J., Correas-Gonzalez, M., Das, S., Moreno, A.D., Drenkhan, F., Fischer, M., Immerzeel, W.W., Izagirre, E., Joshi, R.C., Kougkoulos, I., Knapp, R.K., Li, D., Majeed, U., Matti, S., Moulton, H., Nick, F., Piroton, V., Rashid, I., Reza, M., Ribeiro de Figueiredo, A., Riveros, C., Shrestha, F., Shrestha, M., Steiner, J., Walker-Crawford, N., Wood, J.L., and

665   Yde, J.C.: Progress and challenges in glacial lake outburst flood research (2017-2021): A research community perspective, Nat. Hazards Earth Syst. Sci., 22, 3041-3061, https://doi.org/10.5194/nhess-22-3041-2022, 2022.

Etzelmüller, B., Farbrot, H., Guðmundsson, Á., Humlum, O., Tveito, O.E., and Björnsson, H.: The regional distribution of mountain permafrost in Iceland, Permafrost Periglac., 18, 185–199, https://doi.org/10.1002/ppp.583, 2007.

670   Etzelmüller, B., Patton, H., Schomacker, A., Czekirda, J., Girod, L., Hubbard, A., Lilleøren, K.S., and Westermann, S.: Icelandic permafrost dynamics since the Last Glacial Maximum – model results and geomorphological implications, Quaternary Sci. Rev., 233, 106236, https://doi.org/10.1016/j.quascirev.2020.106236, 2020.

675   Evans, S.G. and Clague, J.J.: Recent climatic change and catastrophic geomorphic processes in mountain environments, Geomorphology, 10, 107-128, https://doi.org/10.1016/0169-555X(94)90011-6, 1994.

Evans, D.J.A. and Twigg, D.R.: The active temperate glacial landsystem: A model based on Breiðamerkurjökull and Fjallsjökull, Iceland, Quaternary Sci. Rev., 21, 2143–2177, https://doi.org/10.1016/S0277-3791(02)00019-7, 2002.

680   Evans, S.G., Scarascia Mugnozza, G., Strom, A. L., Hermanns, R.L., Ischuk, A., and Vinnichenko, S.: Landslides from massive rock slope failure and associated phenomena, in: Landslides from Massive Rock Slope Failure, NATO Science Series, vol. 49, edited by: S.G. Evans, Scarascia Mugnozza, G., Strom, A.L., and Hermanns, R.L., Springer, 3-52, https://doi.org/10.1007/978-1-4020-4037-5_1, 2006.

Flowers, G.E., Marshall, S.J., Björnsson, H., and Clarke, G.K.C.: Sensitivity of Vatnajökull ice cap hydrology and dynamics
685   to climate warming over the next 2 centuries, J. Geophys. Res.-Earth, 110, F02011, https://doi.org/10.1029/2004JF000200, 2005.

Frey, H., Haeberli, W., Linsbauer, A., Huggel, C., and Paul, F.: A multi-level strategy for anticipating future glacier lake formation and associated hazard potentials, Nat. Hazards Earth Syst. Sci., 10, 339–352, https://doi.org/10.5194/nhess-
690   10-339-2010, 2010.

Frey, H., Huggel, C., Chisolm, R.E., Baer, P., McArdell, B., Cochachin, A., and Portocarrero, C.: Multi-source glacial lake outburst flood hazard assessment and mapping for Huaraz, Cordillera Blanca, Peru, Front. Earth Sci., 6, 210, https://doi.org/10.3389/feart.2018.00210, 2018.

695

Geertsema, M., Menounos, B., Bullard, G., Carrivick, J.L., Clague, J.J., Dai, C., Donati, D., Ekstrom, G., Jackson, J.M., Lynett, P., Pichierri, M., Pon, A., Shugar, D.H., Stead, D., Del Bel Belluz, J., Friele, P., Giesbrecht, I., Heathfield, D., Millard, T., Nasonova, S., Schaeffer, A.J., Ward, B.C., Blaney, D., Blaney, E., Brillon, C., Bunn, C., Floyd, W., Higman, B., Hughes, K.E., McInnes, W., Mukherjee, K., and Sharp, M.A.: The 28 November 2020 landslide, tsunami, and outburst
700   flood – a hazard cascade associated with rapid deglaciation at Elliot Creek, British Columbia, Canada, Geophys. Res. Lett., 49, e2021GL096716, https://doi.org/10.1029/2021GL096716, 2022.

Golden Software, LLC: Surfer®, version 13, https://www.goldensoftware.com, 2015.

705   Grab, M., Mattea, E., Bauder, A., Huss, M., Rabenstein, L., Hodel, E., Linsbauer, A., Langhammer, L., Schmid, L., Church, G., Hellmann, S., Délèze, K., Schaer, P., Lathion, P., Farinotti, D., and Maurer, H.: Ice thickness distribution of all Swiss glaciers based on extended ground-penetrating radar data and glaciological modeling, J. Glaciol., 67, 1074–1092, https://doi.org/10.1017/jog.2021.55, 2021.

710   Gruber, S. and Haeberli, W.: Permafrost in steep bedrock slopes and its temperature-related destabilization following climate change, J. Geophys. Res.-Earth, 112, F02S18, https://doi.org/10.1029/2006JF000547, 2007.

Guðmundsson, S., Björnsson, H., Pálsson, F., Magnússon, E., Sæmundsson, Þ., and Jóhannesson, T.: Terminus lakes on the south side of Vatnajökull ice cap, SE-Iceland, Jökull, 69, 1–34, https://doi.org/10.33799/jokull2019.69.001, 2019.

715 Gylfadóttir, S.S., Kim, J., Helgason, J.K., Brynjólfsson, S., Höskuldsson, Á., Jóhannesson, T., Harbitz, C.B., and Løvholt, F.: The 2014 Lake Askja rockslide-induced tsunami: Optimization of numerical tsunami model using observed data, J. Geophys. Res.-Oceans, 122, 4110–4122, https://doi.org/10.1002/2016JC012496, 2017.

Haeberli, W., Buetler, M., Huggel, C., Friedli, T.L., Schaub, Y., and Schleiss, A.J.: New lakes in deglaciating high-mountain regions – opportunities and risks, Clim. Change, 139, 201–214, https://doi.org/10.1007/s10584-016-1771-5, 2016.

720

Haeberli, W., Schaub, Y., and Huggel, C.: Increasing risks related to landslides from degrading permafrost into new lakes in de-glaciating mountain ranges, Geomorphology, 293, 405–417, https://doi.org/10.1016/j.geomorph.2016.02.009, 2017.

Hannesdóttir, H. and Guðmundsson, S.: Glacier outlines, Jöklavefsjá, https://islenskirjoklar.is, 2024.

725

Hannesdóttir, H., Björnsson, H., Pálsson, F., Aðalgeirsdóttir, G., and Guðmundsson, Sv.: Changes in the southeast Vatnajökull ice cap, Iceland, between ~1890 and 2010, Cryosphere, 9, 565–585, https://doi.org/10.5194/tc-9-565-2015, 2015.

Hannesdóttir, H., Sigurðsson, O., Þrastarson, R.H., Guðmundsson, S., Belart, J.M.C., Pálsson, F., Magnússon, E., Víkingsson, S., Kaldal, I., and Jóhannesson, T.: A national glacier inventory and variations in glacier extent in Iceland from the Little Ice Age maximum to 2019, Jökull, 70, 1–34, https://doi.org/10.33799/jokull.70.001, 2020.

730

Harbitz, C.B., Glimsdal, S., Løvholt, F., Kveldsvik, V., Pedersen, G.K., and Jensen, A.: Rockslide tsunamis in complex fjords: From an unstable rock slope at Åkerneset to tsunami risk in western Norway, Coast. Eng., 88, 101–122, https://doi.org/10.1016/j.coastaleng.2014.02.003, 2014.

735 Haritashya, U.K., Kargel, J.S., Shugar, D.H., Leonard, G.J., Strattman, K., Watson, C.S., Shean, D., Harrison, S., Mandli, K.T., and Regmi, D.: Evolution and controls of large glacial lakes in the Nepal Himalaya, Remote Sens., 10, 798, https://doi.org/10.3390/rs10050798, 2018.

Harrison, S., Glasser, N., Winchester, V., Haresign, E., Warren, C., and Jansson, K.: A glacial lake outburst flood associated with recent mountain glacier retreat, Patagonian Andes, Holocene, 16, 611–620, https://doi.org/10.1191/0959683606hl957rr, 2006.

740

Harrison, S., Kargel, J.S., Huggel, C., Reynolds, J., Shugar, D.H., Betts, R.A., Emmer, A., Glasser, N., Haritashya, U.K., Klimeš, J., Reinhardt, L., Schaub, Y., Wiltshire, A., Regmi, D., and Vilímek, V.: Climate change and the global pattern of moraine-dammed glacial lake outburst floods, Cryosphere, 12, 1195–1209, https://doi.org/10.5194/tc-12-1195-2018, 2018.

745

Hartmeyer, I., Delleske, R., Keuschnig, M., Krautblatter, M., Lang, A., Schrott, L., and Otto, J.-C.: Current glacier recession causes significant rockfall increase: The immediate paraglacial response of deglaciating cirque walls, Earth Surf. Dynam., 8, 729–751, https://doi.org/10.5194/esurf-8-729-2020, 2020.

750

Hauksdóttir, H., Helgadóttir, E.G., and Guðmundsson, S.: Jarðfræðikortlagning á Breiðamerkursandi, Final report to the Student Innovation Fund, Náttúrustofa Suðausturlands, Höfn, Iceland, 26 pp., 2021.

755 Hermanns, R.L., Blikra, L.H., Naumann, M., Nilsen, B., Panthi, K.K., Stromeyer, D., and Longva, O.: Examples of multiple rock-slope collapses from Köfels (Ötz valley, Austria) and western Norway, Eng. Geol., 83, 94–108, https://doi.org/10.1016/j.enggeo.2005.06.026, 2006.

760 Hermanns, R.L., Blikra, L.H., Anda, E., Saintot, A., Dahle, H., Oppikofer, T., Fischer, L., Bunkholt, H., Böhme, M., Dehls, J.F., Lauknes, T.R., Redfield, T.F., Osmundsen, P.T., and Eiken, T.: Systematic mapping of large unstable rock slopes in Norway, in: Landslide Science and Practice, vol. 1, edited by: Margottini, C., Canuti, P., and Sassa, K., Springer, 29-34, https://doi.org/10.1007/978-3-642-31325-7_3, 2013.

Hermanns, R.L., Penna, I.M., Oppikofer, T., Noël, F., and Velardi, G.: Rock avalanche, in: Treatise on Geomorphology, vol. 5, 2nd ed., edited by: Shroder, J.F., Elsevier, 85–105, https://doi.org/10.1016/B978-0-12-818234-5.00183-8, 2022.

765 Higman, B., Shugar, D.H., Stark, C.P., Ekström, G., Koppes, N.M., Lynett, P., Dufresne, A., Haeussler, P.J., Geertsema, M., Gulick, S., Mattox, A., Venditti, J.G., Walton, M.A.L., McCall, N., Mckittrick, E., MacInnes, B., Bilderback, E.L., Tang, H., Willis, M.J., Richmond, B., Reece, R.S., Larsen, C., Olson, B., Capra, J., Ayca, A., Bloom, C., Williams, H., Bonno, D., Weiss, R., Keen, A., Skanavis, V., and Loso, M.: The 2015 landslide and tsunami in Taan Fiord, Alaska, Sci. Rep., 8, 12993, https://doi.org/10.1038/s41598-018-30475-w, 2018.

770
Hock, R., Bliss, A., Marzeion, B.E.N., Giesen, R.H., Hirabayashi, Y., Huss, M., Radić, V., and Slangen, A.B.A.: GlacierMIP - A model intercomparison of global-scale glacier mass-balance models and projections, J. Glaciol., 65, 453–467, https://doi.org/10.1017/jog.2019.22, 2019.

Hosmann, S.L., Fabbri, S.C., Buechi, M.W., Hilbe, M., Bauder, A., and Anselmetti, F.S.: Exploring beneath the retreating
775 ice: swath bathymetry reveals sub- to proglacial processes and longevity of future alpine glacial lakes, Ann. Glaciol., 1–6, https://doi.org/10.1017/aog.2024.18, 2024.

Howarth, P.J. and Price, R.J.: The Proglacial lakes of Breiðamerkurjökull and Fjallsjökull, Iceland, Geogr. J., 135, 573–581, https://doi.org/10.2307/1795105, 1969.

780 Howat, I.M. and Eddy, A.L.: Multi-decadal retreat of Greenland's marine-terminating glaciers, J. Glaciol., 57, 389–396, https://doi.org/10.3189/002214311796905631, 2011.

Hubbard, B., Heald, A., Reynolds, J.M., Quincey, D., Richardson, S.D., Luyo, M.Z., Portilla, N.S., and Hambrey, M.J.: Impact of a rock avalanche on a moraine-dammed proglacial lake: Laguna Safuna Alta, Cordillera Blanca, Peru, Earth Surf.
785 Proc. Land., 30, 1251–1264, https://doi.org/10.1002/esp.1198, 2005.

Huggel, C., Kääb, A., Haeberli, W., Teysseire, P., and Paul, F.: Remote sensing based assessment of hazards from glacier lake outbursts: A case study in the Swiss Alps, Can. Geotech. J., 39, 316–330, https://doi.org/10.1139/t01-099, 2002.

790 Hugonnet, R., McNabb, R., Berthier, E., Menounos, B., Nuth, C., Girod, L., Farinotti, D., Huss, M., Dussaillant, I., Brun, F., and Kääb, A.: Accelerated global glacier mass loss in the early twenty-first century, Nature, 592, 726–731, https://doi.org/10.1038/s41586-021-03436-z, 2021.

Hungr, O., Leroueil, S., and Picarelli, L.: The Varnes classification of landslide types, an update, Landslides, 11, 167–194, https://doi.org/10.1007/s10346-013-0436-y, 2014.

795 Icelandic Meteorological Office: Self service of weather observations, delivery no. 2024-06-04 13:08:24, 2024.

Jóhannesson, T., Björnsson, H., Magnússon, E., Guðmundsson, S., Pálsson, F., Sigurðsson, O., Thorsteinsson, T., and Berthier, E.: Ice-volume changes, bias estimation of mass-balance measurements and changes in subglacial lakes derived by lidar mapping of the surface of Icelandic glaciers, Ann. Glaciol., 54, 63–74, https://doi.org/10.3189/2013AoG63A422, 2013.

800

Jóhannesson, T., Pálmason, B., Hjartarson, Á., Jarosch, A.H., Magnússon, E., Belart, J.M.C., and Guðmundsson, M.T.: Non-surface mass balance of glaciers in Iceland, J. Glaciol., 66, 685–697, https://doi.org/10.1017/jog.2020.37, 2020.

Kapitsa, V., Shahgedanova, M., Kasatkin, N., Severskiy, I., Kasenov, M., Yegorov, A., and Tatkova, M.: Bathymetries of
805   proglacial lakes: A new data set from the northern Tien Shan, Kazakhstan, Front. Earth Sci., 11, 1192719, https://doi.org/10.3389/feart.2023.1192719, 2023.

Keefer, D.K.: Landslides caused by earthquakes, Bull. Geol. Soc. Am., 95, 406–421, 1984.

Kershaw, J.A., Clague, J.J., and Evans, S.G.: Geomorphic and sedimentological signature of a two-phase outburst flood from moraine-dammed Queen Bess Lake, British Columbia, Canada, Earth Surf. Proc. Land., 30, 1–25,
810   https://doi.org/10.1002/esp.1122, 2005.

Kjartansson, G.: The Steinholtshlaup, central-south Iceland on January 15th, 1967, Jökull, 17, 249–262, 1967.

Korup, O. and Dunning, S.: Catastrophic mass wasting in high mountains, in: The High-Mountain Cryosphere: Environmental Changes and Human Risks, edited by: Huggel, C., Carey, M., Clague, J.J., and Kääb, A., Cambridge University Press,
815   127-146, https://doi.org/10.1017/CBO9781107588653.008, 2015.

Korup, O. and Tweed, F.: Ice, moraine, and landslide dams in mountainous terrain, Quaternary Sci. Rev., 26, 3406–3422, https://doi.org/10.1016/j.quascirev.2007.10.012, 2007.

Kos, A., Amann, F., Strozzi, T., Delaloye, R., von Ruette, J., and Springman, S.: Contemporary glacier retreat triggers a
820   rapid landslide response, Great Aletsch Glacier, Switzerland, Geophys. Res. Lett., 43, 12,466-12,474, https://doi.org/10.1002/2016GL071708, 2016.

Krautblatter, M. and Leith, K.: Glacier- and permafrost-related slope instabilities, in: The High-Mountain Cryosphere: Environmental Changes and Human Risks, edited by: Huggel, C., Carey, M., Clague, J.J., and Kääb, A., Cambridge University Press, 147-165, https://doi.org/10.1017/CBO9781107588653.009, 2015.
825

Lacroix, P., Belart, J.M.C., Berthier, E., Sæmundsson, Þ., and Jónsdóttir, K.: Mechanisms of landslide destabilization induced by glacier-retreat on Tungnakvíslarjökull area, Iceland, Geophys. Res. Lett., 49, e2022GL098302, https://doi.org/10.1029/2022GL098302, 2022.

830   Lala, J.M., Rounce, D.R., and McKinney, D.C.: Modeling the glacial lake outburst flood process chain in the Nepal Himalaya: Reassessing Imja Tsho's hazard, Hydrol. Earth Syst. Sci., 22, 3721–3737, https://doi.org/10.5194/hess-22-3721-2018, 2018.

Landmælingar Íslands: ÍslandsDEM, https://www.lmi.is, 2021.
835

Landmælingar Íslands: Aerial photo gallery, https://www.lmi.is, last access: 12 August 2022.

Larsen, I.J. and Lamb, M.P.: Progressive incision of the Channeled Scablands by outburst floods, Nature, 538, 229–232, https://doi.org/10.1038/nature19817, 2016.

Lea, J.M., Mair, D.W.F., and Rea, B.R.: Evaluation of existing and new methods of tracking glacier terminus change, J.
840   Glaciol., 60, 323–332, https://doi.org/10.3189/2014JoG13J061, 2014.

Linsbauer, A., Frey, H., Haeberli, W., Machguth, H., Azam, M.F., and Allen, S.: Modelling glacier-bed overdeepenings and possible future lakes for the glaciers in the Himalaya-Karakoram region, Ann. Glaciol., 57, 119–130, https://doi.org/10.3189/2016AoG71A627, 2016.

845

Loftmyndir ehf.: https://www.loftmyndir.is, aerial photographs from 2003, 2025, 2019, and 2021, last access: 30 November 2022.

Loriaux, T. and Casassa, G.: Evolution of glacial lakes from the Northern Patagonia Icefield and terrestrial water storage in a sea-level rise context, Global Planet. Change, 102, 33–40, https://doi.org/10.1016/j.gloplacha.2012.12.012, 2013.

850   Lützow, N., Veh, G., and Korup, O.: A global database of historic glacier lake outburst floods, Earth Syst. Sci. Data, 15, 2983–3000, https://doi.org/10.5194/essd-15-2983-2023, 2023.

Magnin, F., Haeberli, W., Linsbauer, A., Deline, P., and Ravanel, L.: Estimating glacier-bed overdeepenings as possible sites of future lakes in the de-glaciating Mont Blanc massif (Western European Alps), Geomorphology, 350, 106913,
855   https://doi.org/10.1016/j.geomorph.2019.106913, 2020.

Magnússon, E., Björnsson, H., and Pálsson, F.: Landslag í grennd Kvískerja í fortíð og framtíð: Niðurstöður íssjármælinga á Kvíár-, Hrútár- og Fjallsjökli, Jökull, 57, 83–89, 2007.

860   Magnússon, E., Pálsson, F., Björnsson, H., and Guðmundsson, S.: Removing the ice cap of Öraefajökull central volcano, SE-Iceland: Mapping and interpretation of bedrock topography, ice volumes, subglacial troughs and implications for hazards assessments, Jökull, 62, 131–150, 2012.

Magnússon, E., Pálsson, F., Gudmundsson, M.T., Högnadóttir, T., Rossi, C., Thorsteinsson, T., Ófeigsson, B.G., Sturkell, E.,
865   and Jóhannesson, T.: Development of a subglacial lake monitored with radio-echo sounding: Case study from the eastern Skaftá cauldron in the Vatnajökull ice cap, Iceland, Cryosphere, 15, 3731–3749, https://doi.org/10.5194/tc-15-3731-2021, 2021.

Main, B., Copland, L., Smeda, B., Kochtitzky, W., Samsonov, S., Dudley, J., Skidmore, M., Dow, C., Van Wychen, W.,
870   Medrzycka, D., Higgs, E., and Mingo, L.: Terminus change of Kaskawulsh Glacier, Yukon, under a warming climate: Retreat, thinning, slowdown and modified proglacial lake geometry, J. Glaciol., 69, 936-952, https://doi.org/10.1017/jog.2022.114, 2022.

Marzeion, B., Hock, R., Anderson, B., Bliss, A., Champollion, N., Fujita, K., Huss, M., Immerzeel, W.W., Kraaijenbrink, P., Malles, J.-H., Maussion, F., Radić, V., Rounce, D.R., Sakai, A., Shannon, S., van de Wal, R., and Zekollari, H.:
875   Partitioning the uncertainty of ensemble projections of global glacier mass change, Earth's Future, 8, e2019EF001470, https://doi.org/10.1029/2019EF001470, 2020.

Matti, S. and Ögmundardóttir, H.: Local knowledge of emerging hazards: Instability above an Icelandic glacier, Int. J. Disaster Risk Reduct., 58, 102187, https://doi.org/10.1016/j.ijdrr.2021.102187, 2021.

880   Matti, S., Cullen, M., Reichardt, U., and Vigfúsdóttir, A.: Planned relocation due to landslide-triggered tsunami risk in recently deglaciated areas, Int. J. Disaster Risk Reduct., 86, 103536, https://doi.org/10.1016/j.ijdrr.2023.103536, 2023.

McColl, S.T.: Paraglacial rock-slope stability, Geomorphology, 153–154, 1–16, https://doi.org/10.1016/j.geomorph.2012.02.015, 2012.

885 Mergili, M., Pudasaini, S.P., Emmer, A., Fischer, J.-T., Cochachin, A., and Frey, H.: Reconstruction of the 1941 GLOF
process chain at Lake Palcacocha (Cordillera Blanca, Peru), Hydrol. Earth Syst. Sci., 24, 93–114,
https://doi.org/10.5194/hess-24-93-2020, 2020.

Minowa, M., Schaefer, M., and Skvarca, P.: Effects of topography on dynamics and mass loss of lake-terminating glaciers in
southern Patagonia, J. Glaciol., published online, 1–18. https://doi.org/10.1017/jog.2023.42, 2023.

890

Mölg, N., Huggel, C., Herold, T., Storck, F., Allen, S., Haeberli, W., Schaub, Y., and Odermatt, D.: Inventory and evolution
of glacial lakes since the Little Ice Age: Lessons from the case of Switzerland, Earth Surf. Proc. Land., 46, 2551–2564,
https://doi.org/10.1002/esp.5193, 2021.

895 Moon, T. and Joughin, I.: Changes in ice front position on Greenland's outlet glaciers from 1992 to 2007, J. Geophys. Res.-
Earth, 113, F02022, https://doi.org/10.1029/2007JF000927, 2008.

Moragues, S., Lenzano, M.G., Jeanneret, P., Gil, V., and Lannutti, E.: Landslide susceptibility mapping in the Northern part
of Los Glaciares National Park, Southern Patagonia, Argentina using remote sensing, GIS and frequency ratio model,
Quaternary Science Advances, 13., 100146, https://doi.org/10.1016/j.qsa.2023.100146, 2024.

900 Morey, S.M., Shobe, C.M., Huntington, K.W., Lang, K.A., Johnson, A.G., and Duvall, A.R.: The lasting legacy of
megaflood boulder deposition in mountain rivers, Geophys. Res. Lett., 51, 1–11,
https://doi.org/10.1029/2023GL105066, 2024.

Motyka, R.J., Neel, S.O., Connor, C.L., and Echelmeyer, K.A.: Twentieth century thinning of Mendenhall Glacier, Alaska,
and its relationship to climate, lake calving, and glacier run-off, Global Planet. Change, 35, 93–112,
905 https://doi.org/10.1016/S0921-8181(02)00138-8, 2002.

Oppikofer, T., Hermanns, R.L., Roberts, N.J., and Böhme, M.: SPLASH: Semi-empirical prediction of landslide-generated
displacement wave run-up heights, Geol. Soc. Spec. Publ., 477, https://doi.org/10.1144/SP477.1, 2018.

Otto, J.-C., Helfricht, K., Prasicek, G., Binder, D., and Keuschnig, M.: Testing the performance of ice thickness models to
estimate the formation of potential future glacial lakes in Austria, Earth Surf. Proc. Land., 47, 723–741,
910 https://doi.org/10.1002/esp.5266, 2022.

Peng, M.: Measuring glacial lake bathymetry using uncrewed surface vehicles, Nature Reviews Earth & Environment, 4, 514,
https://doi.org/10.1038/s43017-023-00420-1, 2023.

915 Penna, I.M., Nicolet, P., Hermanns, R.L., Böhme, M., and Nöel, F.: Preliminary inventory of rock avalanche deposits and their
related sources in Norway. Regional distribution, main features and topographic constraints, Geological Survey of
Norway, Trondheim, Norway, 30 pp., 2022.

Purdie, H., Gomez, C., and Espiner, S.: Glacier recession and the changing rockfall hazard: Implications for glacier tourism,
920 New Zeal. Geogr., 71, 189–202, https://doi.org/10.1111/nzg.12091, 2015.

Purdie, H., Bealing, P., Tidey, E., Gomez, C., and Harrison, J.: Bathymetric evolution of Tasman Glacier terminal lake, New
Zealand, as determined by remote surveying techniques, Global Planet. Change, 147, 1–11,
https://doi.org/10.1016/j.gloplacha.2016.10.010, 2016.

925

Ramsankaran, R., Verma, P., Majeed, U., and Rashid, I.: Kayak-based low-cost hydrographic surveying system: A
demonstration in high altitude proglacial lake associated with Drang Drung Glacier, Zanskar Himalaya, J. Earth Syst.

Sci., 132, 9, https://doi.org/10.1007/s12040-022-02021-w, 2023.

930 Richardson, S.D. and Reynolds, J.M.: An overview of glacial hazards in the Himalayas. Quatern. Int., 65–66, 31–47, https://doi.org/10.1016/S1040-6182(99)00035-X, 2000.

Rinzin, S., Zhang, G., Sattar, A., Wangchuk, S., Allen, S.K., Dunning, S., and Peng, M.: GLOF hazard, exposure, vulnerability, and risk assessment of potentially dangerous glacial lakes in the Bhutan Himalaya, J. Hydrol., 619, 129311, 935 https://doi.org/10.1016/j.jhydrol.2023.129311, 2023.

Roberts, M.J. and Gudmundsson, M.T.: Öræfajökull volcano: Geology and historical floods, in: Volcanogenic floods in Iceland: An assessment of hazards and risks at Öræfajökull and on the Markarfljót outwash plain, edited by: Pagneux, E., Gudmundsson, M.T., Karlsdóttir, S., Roberts, and M.J., IMO, IES-UI, NCIP-DCPEM, Reykjavík, Iceland, 17-44, 940 2015.

Roberts, M.J., Pálsson, F., Gudmundsson, M.T., Björnsson, H., and Tweed, F.S.: Ice-water interactions during floods from Grænalón glacier-dammed lake, Iceland, Ann. Glaciol., 40, 133–138, https://doi.org/10.3189/172756405781813771, 2005.

945

Roberts, N.J., McKillop, R.J., Lawrence, M.S., Psutka, J.F., Clague, J.J., Brideau, M.-A., and Ward, B.C.: Impacts of the 2007 landslide-generated tsunami in Chehalis Lake, Canada, in: Landslide Science and Practice, vol. 6., edited by: Margottini, C., Canuti, P., and Sassa, K., Springer, 133-140, https://doi.org/10.1007/978-3-642-31319-6_19, 2013.

950 Romstad, B., Harbitz, C.B., and Domaas, U.: A GIS method for assessment of rock slide tsunami hazard in all Norwegian lakes and reservoirs, Nat. Hazards Earth Syst. Sci., 9, 353–364, https://doi.org/10.5194/nhess-9-353-2009, 2009.

Rounce, D.R., Hock, R., Maussion, F., Huggonet, R., Kochtitzky, W., Huss, M., Berthier, E., Brinkerhoff, D., Compagno, L., Copland, L., Farinotti, D., Menounos, B., and McNabb, R.W.: Global glacier change in the 21st century: Every increase 955 in temperature matters, Science, 379, 78–83, https://doi.org/10.1126/science.abo1324, 2023.

Russell, A.J., Roberts, M.J., Fay, H., Marren, P.M., Cassidy, N.J., Tweed, F.S., and Harris, T.: Icelandic jökulhlaup impacts: Implications for ice-sheet hydrology, sediment transfer and geomorphology, Geomorphology, 75, 33–64, https://doi.org/10.1016/j.geomorph.2005.05.018, 2006.

Sattar, A., Goswami, A., Kulkarni, A.V., Emmer, A., Haritashya, U.K., Allen, S., Frey, H., and Huggel, C.: Future Glacial 960 Lake Outburst Flood (GLOF) hazard of the South Lhonak Lake, Sikkim Himalaya, Geomorphology, 388, 107783, https://doi.org/10.1016/j.geomorph.2021.107783, 2021.

Sattar, A., Allen, S., Mergili, M., Haeberli, W., Frey, H., Kulkarni, A.V., Haritashya, U.K., Huggel, C., Goswami, A., and Ramsankaran, R.: Modeling potential glacial lake outburst flood process chains and effects from artificial lake-level 965 lowering at Gepang Gath Lake, Indian Himalaya, J. Geophys. Res.-Earth, 128, e2022JF006826, https://doi.org/10.1029/2022JF006826, 2023.

Sæmundsson, Þ., Sigurðsson, I.A., Pétursson, H.G., Jónsson, H.P., Decaulne, A., Roberts, M.J., and Jensen, E.H.: Bergflóðið sem féll á Morsárjökul 20. mars 2007, Náttúrufræðingurinn, 81, 131–141, 2011.

Schmidt, L.S., Aðalgeirsdóttir, G., Pálsson, F., Langen, P.L., Guðmundsson, S., and Björnsson, H.: Dynamic simulations of 970 Vatnajökull ice cap from 1980 to 2300, J. Glaciol., 66, 97–112, https://doi.org/10.1017/jog.2019.90, 2020.

Schomacker, A.: Expansion of ice-marginal lakes at the Vatnajökull ice cap, Iceland, from 1999 to 2009, Geomorphology, 119, 232–236, https://doi.org/10.1016/j.geomorph.2010.03.022, 2010.

975   Shugar, D.H., Burr, A., Haritashya, U.K., Kargel, J.S., Watson, C.S., Kennedy, M.C., Bevington, A.R., Betts, R.A., Harrison, S., and Strattman, K.: Rapid worldwide growth of glacial lakes since 1990, Nat. Clim. Change, 10, 939–945, https://doi.org/10.1038/s41558-020-0855-4, 2020.

Shugar, D.H., Jacquemart, M., Shean, D., Bhushan, S., Upadhyay, K., Sattar, A., Schwanghart, W., McBride, S., Van Wyk de
980   Vries, M., Mergili, M., Emmer, A., Deschamps-Berger, C., McDonnell, M., Bhambri, R., Allen, S., Berthier, E., Carrivick, J.L., Clague, J.J., Dokukin, M., Dunning, S.A., Frey, H., Gascoin, S., Haritashya, U.K., Huggel, C., Kääb, A., Kargel, J.S., Kavanaugh, J.L., Lacroix, P., Petley, D., Rupper, S., Azam, M.F., Cook, S.J., Dimri, A.P., Eriksson, M., Farinotti, D., Fiddes, J., Gnyawali, K.R., Harrison, S., Jha, M., Koppes, M., Kumar, A., Leinss, S., Majeed, U., Mal, S., Muhuri, A., Noetzli, J., Paul, F., Rashid, I., Sain, K., Steiner, J., Ugalde, F., Watson, C.S., and Westoby, M.J.: A massive
985   rock and ice avalanche caused the 2021 disaster at Chamoli, Indian Himalaya, Science, 373, 300-306, https://doi.org/10.1126/science.abh4455, 2021.

Sigurðsson, O. and Williams, R.: Rockslides on the terminus of "Jökulsárgilsjökull", southern Iceland, Geogr. Ann. A, 73, 129–140, https://doi.org/10.2307/521018, 1991.
990

Sosio, R.: Rock–snow–ice avalanches, in: Landslide Hazards, Risks, and Disasters, edited by: Shroder, J.F. and Davies, T., Elsevier, 191-240, https://doi.org/10.1016/B978-0-12-396452-6.00007-0, 2015.

Sosio, R., Crosta, G.B., Chen, J.H., and Hungr, O.: Modelling rock avalanche propagation onto glaciers, Quaternary Sci. Rev., 47, 23–40, https://doi.org/10.1016/j.quascirev.2012.05.010, 2012.

995   Steffen, T., Huss, M., Estermann, R., Hodel, E., and Farinotti, D.: Volume, evolution, and sedimentation of future glacier lakes in Switzerland over the 21st century, Earth Surf. Dynam., 10, 723–741, https://doi.org/10.5194/esurf-10-723-2022, 2022.

Stevenson, J.A., McGarvie, D.W., Smellie, J.L., and Gilbert, J.S.: Subglacial and ice-contact volcanism at the Öræfajökull stratovolcano, Iceland, Bull. Volcanol., 68, 737–752, https://doi.org/10.1007/s00445-005-0047-0, 2006.
1000

Stewart, E.J., Wilson, J., Espiner, S., Purdie, H., Lemieux, C., and Dawson, J.: Implications of climate change for glacier tourism, Tourism Geog., 18, 377–398, https://doi.org/10.1080/14616688.2016.1198416, 2016.

Stoffel, M. and Huggel, C.: Effects of climate change on mass movements in mountain environments, Prog. Phys. Geog., 36,
1005   421–439, https://doi.org/10.1177/0309133312441010, 2012.

Strzelecki, M.C. and Jaskólski, M.W.: Arctic tsunamis threaten coastal landscapes and communities – survey of Karrat Isfjord 2017 tsunami effects in Nuugaatsiaq, western Greenland, Nat. Hazards Earth Syst. Sci., 20, 2521–2534, https://doi.org/10.5194/nhess-20-2521-2020, 2020.
1010

Sutherland, J.L., Carrivick, J.L., Gandy, N., Shulmeister, J., Quincey, D.J., and Cornford, S.L.: Proglacial lakes control glacier geometry and behavior during recession, Geophys. Res. Lett., 47, e2020GL088865, https://doi.org/10.1029/2020GL088865, 2020.

Svennevig, K., Dahl-Jensen, T., Keiding, M., Boncori, J.P.M., Larsen, T.B., Salehi, S., Solgaard, A.M., and Voss, P.H.:
1015   Evolution of events before and after the 17 June 2017 rock avalanche at Karrat Fjord, West Greenland – a multidisciplinary approach to detecting and locating unstable rock slopes in a remote Arctic area, Earth Surf. Dynam., 8, 1021–1038, https://doi.org/10.5194/esurf-8-1021-2020, 2020.

Tang, M., Xu, Q., Wang, L., Zhao, H., Wu, G., Zhou, J., Li, G., Cai, W., and Chen, X.: Hidden dangers of ice avalanches and glacier lake outburst floods on the Tibetan Plateau: identification, inventory, and distribution, Landslides, 20, 2563–2581, https://doi.org/10.1007/s10346-023-02125-4, 2023.

Thorarinsson, S.: The ice dammed lakes of Iceland with particular reference to their values as indicators of glacier oscillations, Geogr. Ann., 21, 216–242, 1939.

Thorarinsson, S.: Vatnajökull: scientific results of the Swedish–Icelandic investigations 1936–37–38. Chapter XI. Oscillations of the Iceland glaciers in the last 250 years, Geogr. Ann., 25, 1–54, 1943.

Welling, J. and Abegg, B.: Following the ice: Adaptation processes of glacier tour operators in Southeast Iceland, Int. J. Biometeorol., 65, 703–715, https://doi.org/10.1007/s00484-019-01779-x, 2021.

Welling, J., Árnason, Þ., and Ólafsdóttir, R.: Implications of climate change on nature-based tourism demand: A segmentation analysis of glacier site visitors in southeast Iceland, Sustainability, 12, 5338, https://doi.org/10.3390/su12135338, 2020.

Wells, G.H., Dugmore, A.J., Beach, T., Baynes, E.R.C., Sæmundsson, Þ., and Luzzadder-Beach, S.: Reconstructing glacial outburst floods (jökulhlaups) from geomorphology: Challenges, solutions, and an enhanced interpretive framework, Prog. Phys. Geog., 46, 398-421, https://doi.org/10.1177/03091333211065001, 2022.

Westoby, M.J., Glasser, N.F., Brasington, J., Hambrey, M.J., Quincey, D.J., and Reynolds, J.M.: Modelling outburst floods from moraine-dammed glacial lakes, Earth-Sci. Rev., 134, 137–159, https://doi.org/10.1016/j.earscirev.2014.03.009, 2014a.

Westoby, M.J., Glasser, N.F., Hambrey, M.J., Brasington, J., Reynolds, J.M., and Hassan, M.A.A.M.: Reconstructing historic Glacial Lake Outburst Floods through numerical modelling and geomorphological assessment: Extreme events in the Himalaya, Earth Surf. Proc. Land., 39, 1675–1692, https://doi.org/10.1002/esp.3617, 2014b.

Wilson, R., Harrison, S., Reynolds, J., Hubbard, A., Glasser, N.F., Wündrich, O., Iribarren Anacona, P., Mao, L., and Shannon, S.: The 2015 Chileno Valley glacial lake outburst flood, Patagonia, Geomorphology, 332, 51–65, https://doi.org/10.1016/j.geomorph.2019.01.015, 2019.

Worni, R., Huggel, C., Clague, J.J., Schaub, Y., and Stoffel, M.: Coupling glacial lake impact, dam breach, and flood processes: A modeling perspective, Geomorphology, 224, 161–176, https://doi.org/10.1016/j.geomorph.2014.06.031, 2014.

Zemp, M., Huss, M., Thibert, E., Eckert, N., McNabb, R., Huber, J., Barandun, M., Machguth, H., Nussbaumer, S.U., Gärtner-Roer, I., Thomson, L., Paul, F., Maussion, F., Kutuzov, S., and Cogley, J.G.: Global glacier mass changes and their contributions to sea-level rise from 1961 to 2016, Nature, 568, 382–386, https://doi.org/10.1038/s41586-019-1071-0, 2019.

Zhang, G., Carrivick, J.L., Emmer, A., Shugar, D.H., Veh, G., Wang, X., Labedz, C., Mergili, M., Mölg, N., Huss, M., Allen, S., Sugiyama, S., and Lützow, N.: Characteristics and changes of glacial lakes and outburst floods, Nature Reviews Earth & Environment, https://doi.org/10.1038/s43017-024-00554-w, 2024.

Þórhallsdóttir, G.: Fjöldi í Vatnajökulsþjóðgarði 2018 til 2022, Vatnajökulsþjóðgarður, Höfn, Iceland, 299 pp., 2023.